

On the robustness of gradient-based MCMC algorithms

Samuel Livingstone^{*1} and Giacomo Zanella^{†2}

¹Department of Statistical Science, University College London.

²Department of Decision Sciences, BIDSa and IGIER, Bocconi University.

May 11, 2022

Abstract

We analyze the tension between robustness and efficiency for Markov chain Monte Carlo (MCMC) sampling algorithms. In particular, we focus on robustness of MCMC algorithms with respect to heterogeneity in the target and their sensitivity to tuning, an issue of great practical relevance but still understudied theoretically. We show that the spectral gap of the Markov chains induced by classical gradient-based MCMC schemes (e.g. Langevin and Hamiltonian Monte Carlo) decays exponentially fast in the degree of mismatch between the scales of the proposal and target distributions, while for the random walk Metropolis (RWM) the decay is linear. This result provides theoretical support to the notion that gradient-based MCMC schemes are less robust to heterogeneity and more sensitive to tuning. Motivated by these considerations, we propose a novel and simple to implement gradient-based MCMC algorithm, inspired by the classical Barker accept-reject rule, with improved robustness properties. Extensive theoretical results, dealing with robustness to heterogeneity, geometric ergodicity and scaling with dimensionality, show that the novel scheme combines the robustness of RWM with the efficiency of classical gradient-based schemes. We illustrate with simulation studies how this type of robustness is particularly beneficial in the context of adaptive MCMC, giving examples in which the new scheme gives orders of magnitude improvements in efficiency over state-of-the-art alternatives.

1 Introduction

Markov chain Monte Carlo (MCMC) is a popular method for calculating high-dimensional integrals, which has become the dominant approach to fitting statistical models in the Bayesian paradigm [Brooks et al., 2011] (and is also widely used in many other fields, e.g. [Krauth, 2006, Stuart, 2010]). The central idea is to construct a Markov chain with limiting distribution the posterior under consideration, and use ergodic averages to approximate expectations of interest. In the celebrated Metropolis–Hastings algorithm, the Markov chain transition is constructed using a combination of a ‘candidate’ kernel, to suggest a possible move at each iteration, together with an accept-reject mechanism [Metropolis et al., 1953, Hastings, 1970]. Many different flavours of Metropolis–Hastings exist, with the most common difference being in the construction of the candidate kernel. In the Random walk Metropolis, proposed moves are generated using a symmetric distribution centred at the current point. Two more sophisticated methods are the Metropolis-adjusted Langevin algorithm [Roberts and Tweedie, 1996] and Hamiltonian/hybrid Monte Carlo [Duane et al., 1987, Neal, 2011]. Both use gradient information about the posterior to inform proposals. Gradient-based methods are widely considered to be state-of-the-art in

^{*}samuel.livingstone@ucl.ac.uk

[†]giacomo.zanella@unibocconi.it

MCMC, and much current work has been dedicated to their study and implementation (e.g. Beskos et al. [2013], Durmus and Moulines [2017], Dalalyan [2017]).

Several measures of performance have been developed to help choose a suitable candidate kernel for a given task. One of these is high-dimensional scaling arguments, which compare how the efficiency decays with d , the dimension of the state space. For the random walk algorithm this decay is of the order d^{-1} [Roberts et al., 1997], while for the Langevin algorithm the same figure is $d^{-1/3}$ [Roberts and Rosenthal, 1998] and for Hamiltonian Monte Carlo it is $d^{-1/4}$ [Beskos et al., 2013]. Another measure is to find general conditions under which a kernel will produce a geometrically ergodic Markov chain. For the random walk algorithm this essentially occurs when the tails of the posterior decay at a faster than exponential rate and are suitably regular (more precise conditions are given in [Jarner and Hansen, 2000]). The same is broadly true of the Langevin and Hamiltonian schemes [Roberts and Tweedie, 1996, Livingstone et al., 2019, Durmus et al., 2017a], but here there is an additional restriction that the tails should not decay too quickly. This limitation is caused by the way in which gradients are used to construct the candidate kernel, which can result in the algorithm generating unreasonable proposals that are nearly always rejected in certain regions [Roberts and Tweedie, 1996, Livingstone et al., 2019].

There is clearly some tension between the different results presented above. According to the scaling arguments gradient information is preferable. The ergodicity results, however, imply that gradient-based schemes are typically less *robust* than others, in the sense that there is a smaller class of posterior distributions for which the output will be a geometrically ergodic Markov chain. It is natural to wonder whether it is possible to incorporate gradient information in such a way that this measure of robustness is not compromised. Simple approaches to modifying the Langevin algorithm for this purpose have been suggested (based on the idea of truncating gradients, e.g. Roberts and Tweedie [1996], Atchade [2006]), but these typically compromise the favourable scaling of the original method. In addition to this, it is often remarked that gradient-based methods can be difficult to tune. Algorithms performance is often highly sensitive to the choice of scale within the proposal [Neal, 2003, Fig.15], and if this is chosen to be too large performance can degrade rapidly. Because of this, practitioners must spend a long time adjusting the tuning parameters to ensure that the algorithm is running well, or develop sophisticated adaptation schemes for this purpose (e.g. Hoffman and Gelman [2014]). In both cases, considerable computational and design effort is required to tune the algorithms before they start performing as desired. The problem is more severe when the posterior is much more concentrated in some dimensions than others or features strong correlations among parameters. We will refer to this issue as *robustness to tuning* or *robustness to heterogeneity*.

In this article we make two contributions. First, we present a direct argument showing how the spectral gaps for the random walk, Langevin and Hamiltonian algorithms decay as the degree of heterogeneity in the posterior is increased. Our results in Section 2 of the present contribution show that the spectral gaps for gradient-based algorithms typically decay to zero at a faster rate than for the Random walk Metropolis as the mismatch between the proposal and target scales in a given direction increases. This provides an explicit mathematical characterization for the observations of practitioners that gradient-based schemes are more sensitive to tuning. Second, we devise a gradient-based method that retains favourable high-dimensional scaling properties, but in addition shares the desirable robustness properties of the random walk Metropolis, both in terms of geometric ergodicity and robustness to tuning. The new method, which we call *the Barker proposal* scheme (for reasons that will become apparent), is inspired by the concept of ‘locally-balanced’ proposals, introduced in [Zanella, 2019] for discrete state spaces. In Section 3 we generalize the approach to continuous state spaces, and introduce the Barker proposal scheme. In Section 4 we conduct a detailed analysis of the ergodicity, scaling and robustness properties of this new method, establishing that it shares the favourable robustness to tuning of the random walk algorithm, can be geometrically ergodic in the presence of very light tails, and

enjoys the $d^{-1/3}$ scaling with dimension of the Langevin scheme. The theory is then supported by a extensive simulation study in Section 5. Perhaps the most visible advantage of an algorithm being robust to heterogeneity comes when tuning parameters are learned adaptively during sampling. We show in Section 5 that in some realistic modelling scenarios the Barker proposal scheme enjoys several orders of magnitude improvement in terms of effective sample size per gradient evaluation when compared to many state-of-the-art gradient-based samplers in this setting, such as the Metropolis-adjusted Langevin algorithm, its tamed variant [Brosse et al., 2018] and the No-U-Turn sampler [Hoffman and Gelman, 2014]. The code to reproduce the experiments is available from the online repository at the link <https://github.com/gzanela/barker>. Proofs are provided in the supplement.

1.1 Setup and notation

Throughout we work on the Borel space $(\mathbb{R}^d, \mathcal{B})$, with $d \geq 1$ indicating the dimension. We assume that interest lies in computing expectations with respect to some probability measure $\pi(\cdot)$ which has a density $\pi(x)$ that is positive for all $x \in \mathbb{R}^d$, and for which $\log \pi \in C^1(\mathbb{R}^d)$. To employ Markov chain Monte Carlo for this purpose, we choose a Markov transition kernel $P : \mathbb{R}^d \times \mathcal{B} \rightarrow [0, 1]$ in such a way that $\lim_{n \rightarrow \infty} P^n(x, A) = \pi(A)$, for π -almost all $x \in \mathbb{R}^d$ and all $A \in \mathcal{B}$. Then, after choosing a starting point $X^{(0)}$, successive samples $X^{(t)} | X^{(t-1)} \sim P(X^{(t-1)}, \cdot)$ can be drawn for $t \in \{1, \dots, N\}$, and for some function of interest f the expectation $\mathbb{E}_\pi f$ can be approximated by the ergodic average $\sum_{t=M+1}^N f(X^{(t)}) / (N - M)$ for some suitably chosen $M \in \mathbb{N}$.

The Markov chains we consider will be of the Metropolis–Hastings type, meaning that we first define a candidate kernel $Q : \mathbb{R}^d \times \mathcal{B} \rightarrow [0, 1]$, and then set

$$P(x, dy) := \alpha(x, y)Q(x, dy) + r(x)\delta_x(dy), \quad (1.1)$$

where

$$\alpha(x, y) := \min \left(1, \frac{\pi(dy)Q(y, dx)}{\pi(dx)Q(x, dy)} \right) \quad (1.2)$$

is the *acceptance rate* for a proposal y given the current point x (provided that the expression is well-defined, see Tierney [1998] for details here), and $r(x) := 1 - \int \alpha(x, y)Q(x, dy)$ is the average probability of rejection given that the current point is x . It is straightforward to establish that such a P produces a Markov chain which is π -invariant, and provided Q and $\pi(\cdot)$ satisfy certain conditions (e.g. Roberts and Rosenthal [2004]), that $\pi(\cdot)$ is the limiting distribution for the chain. An example implementation is given in Section 2. A Markov chain is called *geometrically ergodic* if

$$\|P^t(x, \cdot) - \pi(\cdot)\|_{TV} \leq CV(x)\rho^t, \quad t \geq 1, \quad (1.3)$$

for some $C < \infty$, Lyapunov function $V : \mathbb{R}^d \rightarrow [1, \infty)$, and $\rho < 1$, where $\|\mu(\cdot) - \nu(\cdot)\|_{TV} := \sup_{A \in \mathcal{B}} |\mu(A) - \nu(A)|$ for probability measures $\mu(\cdot)$ and $\nu(\cdot)$. When such a condition can be established for a reversible Markov chain, then a Central Limit Theorem exists for any square-integrable function [Roberts and Rosenthal, 2004].

We will need the following notational conventions. For two functions $f, g : \mathbb{R} \rightarrow \mathbb{R}$, we use the Bachmann–Landau notation $f(t) = \Theta(g(t))$ if there are finite positive constants c and C such that

$$\liminf_{t \rightarrow \infty} \frac{f(t)}{g(t)} = c, \quad \text{and} \quad \limsup_{t \rightarrow \infty} \frac{f(t)}{g(t)} = C.$$

For $h \in \mathbb{R}$, we also write $h \uparrow \infty$ and $h \downarrow 0$ to emphasize the direction of convergence when this is important.

2 Robustness to heterogeneity

Consider a family of distributions indexed by $\lambda > 0$ with densities

$$\pi^{(\lambda)}(x) = \lambda^{-1} \pi(x_1/\lambda, x_2, \dots, x_d), \quad x = (x_1, \dots, x_d) \in \mathbb{R}^d. \quad (2.1)$$

The $\lambda \downarrow 0$ regime is representative of distributions in which one component (in this case the first) has a very small scale compared to all others. Conversely the $\lambda \uparrow \infty$ regime reflects the case in which one component has a much larger scale than its counterparts. In either situation, targeting the distribution with a Metropolis–Hastings algorithm for which the chosen candidate kernel has the same scale in every component will be a suboptimal strategy. In this section we consider these two regimes for the random walk, Langevin and Hamiltonian schemes, and in each case quantify how suboptimal such a strategy is. Intuitively, we can think of λ as a parameter quantifying the mismatch between proposal and target scales in the first coordinate.

For simplicity of exposition, we prefer to work with the equivalent problem in which the distribution of interest consists of components that have fixed scales, and instead the candidate kernel is altered in the first component. As a concrete example, consider the Gaussian Random Walk Metropolis algorithm. Here we construct a Markov chain by doing the following for $t = 0, \dots, T - 1$, given the starting point $x^{(0)} \in \mathbb{R}^d$ and a distribution of interest $\pi(\cdot)$.

1. Propose $y = x^{(t)} + \xi$, where $\xi \sim N(0, \Sigma^{(h)})$ for some $\Sigma^{(h)} \in \mathbb{R}^{d \times d}$
2. Set $x^{(t+1)} = y$ with probability $\alpha(x^{(t)}, y)$, otherwise set $x^{(t+1)} = x^{(t)}$, where

$$\alpha(x^{(t)}, y) = \min \left\{ 1, \frac{\pi(y)}{\pi(x^{(t)})} \right\}.$$

If we set

$$\Sigma^{(h)} = \sigma^2 \begin{pmatrix} h^2 & \dots & 0 \\ \vdots & \ddots & \vdots \\ 0 & \dots & 1 \end{pmatrix},$$

where $\Sigma_{ii}^{(h)}/\sigma^2 = 1$ if $i > 1$ and $\Sigma_{ij}^{(h)} = 0$ if $i \neq j$, then letting $h \uparrow \infty$ leads to the scenario in which a step-size that is too large is being used for the first component, and letting $h \downarrow 0$ gives the opposite case. Setting $h := 1/\lambda$ gives the equivalence with (2.1).

This measure of robustness has a clear practical interpretation. If a user is choosing the step-size of an algorithm by hand, then it gives information on how much time should be invested in initial testing to ensure that a good choice has been made. If instead the tuning parameters are selected using some adaptive mechanism, then efficient sampling can only begin to take place once the adaptation has stabilised. We show in Section 5 that if an algorithm is robust to heterogeneity then this process can be orders of magnitude quicker than in the alternative case, which can have profound consequences for the performance and computational cost of an adaptive method. See Section 2.3 for discussion on possible extensions of this framework.

2.1 The large h regime

In this section we assess the robustness to heterogeneity of random walk, Langevin and Hamiltonian Metropolis–Hastings schemes as $h \uparrow \infty$. Our measure of performance will be the spectral gap of the resulting Markov chain. Consider the space of functions

$$L_{0,1}^2(\pi) = \{f : \mathbb{R}^d \rightarrow \mathbb{R} \mid \mathbb{E}_\pi[f] = 0, \text{Var}_\pi[f] = 1\}.$$

Note that any function g with $\mathbb{E}_\pi g^2 < \infty$ can be associated with an $f \in L_{0,1}^2(\pi)$ through the map $f = (g - \mathbb{E}_\pi g)/\sqrt{\text{Var}_\pi g}$, and that if $X^{(t)} \sim \pi(\cdot)$ and $X^{(t+1)}|X^{(t)} \sim P(X^{(t)}, \cdot)$ then

$$\text{Corr}\{g(X^{(t)}), g(X^{(t+1)})\} = \text{Corr}\{f(X^{(t)}), f(X^{(t+1)})\}.$$

The (right) spectral gap of a π -reversible Markov chain with transition kernel P is

$$\text{Gap}(P) = \inf_{f \in L^2_{0,1}(\pi)} \frac{1}{2} \int (f(y) - f(x))^2 \pi(dx) P(x, dy). \quad (2.2)$$

The expression inside the infimum is called a *Dirichlet form*, and can be thought of as the ‘expected squared jump distance’ for the function f provided the chain is stationary. This can in turn be re-written

$$1 - \text{Corr}\{f(X^{(t)}), f(X^{(t+1)})\}.$$

Maximising the spectral gap of a reversible Markov chain can therefore be understood as minimising the *worst-case* first-order autocorrelation among all possible square-integrable test functions.

The spectral gap allows to bound the variances of ergodic averages (see Proposition 1 of Rosenthal, 2003). Also, a direct connection between the spectral gap and mixing properties of the chain can be made if the operator $Pf(x) := \int f(y)P(x, dy)$ is positive on $L^2(\pi)$. This will always be the case if the chain is made lazy, which is the approach taken in Woodard et al. [2009], and the same adjustment can be made here if desired. Spectral gaps are also naturally relatable to the size or level of difficulty of the problem at hand. For example, if the spectral gap decays polynomially as this level of difficulty increases then the chain is said to be *rapid mixing*, and if exponentially then it is said to be *torpid mixing* (e.g. Woodard et al. [2009]). The results presented here can be thought of in the same spirit.

2.1.1 Random walk Metropolis

In the Random Walk Metropolis, given a current point $x \in \mathbb{R}^d$, a proposal y is calculated using the equation

$$y = x + \sigma\xi, \quad (2.3)$$

with $\xi \sim \mu(\cdot)$ for some centred symmetric distribution $\mu(\cdot)$, and $\sigma > 0$. We write Q^R for a candidate kernel that generates such proposals, and P^R for the resulting Metropolis–Hastings transition. Here we only consider kernels of the form $Q^R(x, dy) = q^R(x, y)dy$, where q^R is a probability density for any fixed x . Random walk candidate kernels are those for which $q^R(x, y) = \sigma^{-d}\mu((y - x)/\sigma) = \sigma^{-d}\mu((x - y)/\sigma) = q^R(y, x)$, where $\mu(\xi)$ denotes the density corresponding to the measure $\mu(\cdot)$. As a consequence $\alpha(x, y) = \min(1, \pi(y)/\pi(x))$.

To state the main result of this subsection, we must introduce the transition kernel P_h^R . Take a Random Walk Metropolis kernel P^R with associated candidate density $q^R(x, y) = \sigma^{-d}\mu((y - x)/\sigma)$, for which the $\sigma > 0$ is fixed. Write $\delta = y - x = (y_1 - x_1, \dots, y_d - x_d)$, and set

$$\delta_h := \left(\frac{y_1 - x_1}{h}, y_2 - x_2, \dots, y_d - x_d \right). \quad (2.4)$$

We introduce the density

$$q_h^R(x, y) := \frac{1}{h\sigma^d} \mu\left(\frac{\delta_h}{\sigma}\right), \quad (2.5)$$

and define P_h^R to be the random walk Metropolis kernel with candidate kernel $Q_h^R(x, dy) := q_h^R(x, y)dy$. Setting $h = 1$ gives $P_h^R = P^R$, but in general the scale of the first component of the resulting proposal will be $h\sigma$. Letting $h \uparrow \infty$ therefore gives the regime in which an overly large step-size is used for the first component.

We impose the following regularity condition on the density $\mu(\xi)$, which is satisfied for most popular choices of μ , as shown in the subsequent proposition.

Condition 2.1. *There exists $h_0 \geq 1$ such that for any $x, y \in \mathbb{R}^d$ and $h > h_0$*

$$\mu(\delta_h) \geq \mu(\delta), \quad (2.6)$$

with $\delta = y - x$ and δ_h as in (2.4). In addition, $\sup_{z \in \mathbb{R}^d} \mu(z) < \infty$.

Proposition 2.1. *Condition 2.1 holds in each of the below cases:*

- (i) $q^R(x, y) = (2\pi\sigma^2)^{-d/2} \exp(-\|x - y\|_2^2/(2\sigma^2))$ (Gaussian)
- (ii) $q^R(x, y) = 2^{-d} \exp(-\|x - y\|_1)$ (Laplace)
- (iii) $q^R(x, y) \propto (1 + \|y - x\|_2^2/\nu)^{-(\nu+d)/2}$ for $\nu \in \{1, 2, \dots\}$ (Student's t)

We conclude the section with a characterization of the rate of convergence to zero of the spectral gap for the Random Walk Metropolis as $h \uparrow \infty$.

Theorem 2.1. *Assume Condition 2.1 and $\text{Gap}(P^R) > 0$. Then it holds that*

$$\text{Gap}(P_h^R) = \Theta(h^{-1}), \quad \text{as } h \uparrow \infty.$$

Note that Theorem 2.1 requires virtually no assumptions on the target π apart from $\text{Gap}(P^R) > 0$.

2.1.2 Metropolis-adjusted Langevin algorithm

In the Langevin algorithm, given the current point $x \in \mathbb{R}^d$, a proposal y is generated by setting

$$y = x + \frac{\sigma^2}{2} \nabla \log \pi(x) + \sigma \xi,$$

for some $\sigma > 0$ and $\xi \sim N(0, I)$. In this case the proposal is no longer symmetric and so the full Hastings ratio (1.2) must be used. The proposal mechanism is based on the overdamped Langevin stochastic differential equation $dX_t = \nabla \log \pi(X_t)dt + \sqrt{2}dB_t$. We write Q^M and P^M for the corresponding candidate and Metropolis–Hastings kernels.

As in the previous section, to discuss how spectral gaps depend on the step-size, we introduce the kernels Q_h^M and P_h^M , for which the first component is generated/proposed using the rule $y_1 = x_1 + (h\sigma)^2 \partial_1 \log \pi(x)/2 + (h\sigma)\xi_1$ (where $\partial_1 := \partial/\partial x_1$). Again setting $h = 1$ gives $P_h^M = P^M$ and $h \uparrow \infty$ represents the scenario in which an overly large scale is used for the first component.

We present results for the Langevin algorithm in two settings. Initially we consider more restrictive conditions under which our upper bound on the spectral gap depends on the tail behaviour of $\pi(x)$ in a particularly explicit manner, and then give a broader result.

Condition 2.2. *Assume the following:*

- (i) $\pi(\cdot)$ has a density of the form $\pi(x) = \pi_1(x_1)\pi_{2:n}(x_2, \dots, x_d)$.
- (ii) For some $q \in [0, 1)$, it holds that

$$\left| \frac{d}{dx_1} \log \pi_1(x_1) \right| = \Theta(|x_1|^q) \quad \text{as } |x_1| \uparrow \infty. \quad (2.7)$$

Theorem 2.2. *If Condition 2.2 holds, then there is a $\gamma > 0$ such that*

$$\text{Gap}(P_h^M) \leq \Theta\left(e^{-\gamma h^{1+q} - q \log(h)}\right) \quad \text{as } h \uparrow \infty.$$

When compared with the random walk algorithm, Theorem 2.2 shows that the Langevin scheme is much less robust to heterogeneity. Indeed, the spectral gap decays *exponentially fast* in h , meaning that even small errors in the choice of step-size can have large impacts on the algorithm's efficiency and thus practitioners must invest considerable effort tuning the algorithm for good performance, as shown through simulations in Section 5. Theorem 2.2 also illustrates that the Langevin algorithm is more sensitive to h when the tails of $\pi(\cdot)$ are lighter. This is intuitive, as it is in this setting that the gradient terms can become very large in certain regions of the state space.

Remark 2.1. *Theorem 2.2 (and Theorem 2.4 below) could be extended to the case $q \geq 1$ in (2.7), however in these cases samplers typically fail to be geometrically ergodic when h is large [Roberts and Tweedie, 1996, Livingstone et al., 2019] and thus the spectral gap is typically 0 and the theorem becomes trivial.*

Remark 2.2. *Condition 2.2 (ii) could be replaced with the simpler requirement that $\|\nabla \log \pi_1(x_1)\| \uparrow \infty$, with the corresponding bound $\text{Gap}(P_h^M) \leq \Theta(e^{-h})$. We prefer to keep it in this form to be the same as Theorem 2.4.*

A different set of conditions, which hold much more generally, and corresponding upper bound are presented below.

Condition 2.3. *Assume the following:*

(i) *There exist a positive constant γ such that*

$$\liminf_{|x_1| \rightarrow \infty} \left(\inf_{(x_2, \dots, x_d) \in \mathbb{R}^{d-1}} \left| \frac{\partial \log \pi(x)}{\partial x_1} \right| \|x\|^\gamma \right) > 0, \quad (2.8)$$

(ii) *Given $X \sim \pi$ there exist a positive constant β such that*

$$\mathbb{P}(\|X\| > t) \leq \Theta(e^{-t^\beta}) \quad \text{as } t \rightarrow \infty. \quad (2.9)$$

Theorem 2.3. *If Condition 2.3 holds, then as $h \uparrow \infty$*

$$\text{Gap}(P_h^M) \leq \Theta(e^{-h^\alpha})$$

for some $\alpha > 0$.

We expect Condition 2.3 to be satisfied in most commonly encountered scenarios, with the exception of particularly heavy-tailed models. In the exponential family class $\pi(x) \propto \exp\{-\alpha\|x\|^\beta\}$, for example, Condition 2.3 holds for any α and $\beta > 0$ (see proof in the supplement).

2.1.3 Hamiltonian Monte Carlo

In Hamiltonian Monte Carlo we write the current point $x \in \mathbb{R}^d$ as $x(0)$, and construct the proposal $y := x(L)$ for some prescribed integer L using the update

$$x(L) = x(0) + \sigma^2 \left(\frac{L}{2} \nabla \log \pi(x(0)) + \sum_{j=1}^{L-1} (L-j) \nabla \log \pi(x(j)) \right) + L\sigma\xi(0), \quad (2.10)$$

where each $x(j)$ is defined recursively in the same manner, and $\xi(0) \sim N(0, I)$. The transition is based on numerically solving Hamilton's equations for the Hamiltonian system $H(x, \xi) = -\log \pi(x) + \xi^T \xi / 2$ for $L\sigma$ units of time. The decision of whether or not the proposal is accepted is taken using the acceptance probability $\min(1, \pi(y)/\pi(x)e^{-\xi(L)^T \xi(L)/2 + \xi(0)^T \xi(0)/2})$, where

$$\xi(L) = \xi(0) + \frac{\sigma}{2} (\nabla \log \pi(x(0)) + \nabla \log \pi(x(L))) + \sigma \sum_{j=1}^{L-1} \nabla \log \pi(x(j)).$$

A more detailed description is given in Neal [2011]. We write P^H for the corresponding Metropolis–Hastings kernel.

Here we present a heterogeneity result under Condition 2.2 of the previous subsection. Again we must introduce the transition kernel P_h^H , which we do by replacing σ when updating the first component x_1 with σh , precisely as was done for the Langevin scheme.

Theorem 2.4. *If Condition 2.2 holds, then there is a $\gamma > 0$ such that*

$$\text{Gap}(P_h^H) \leq \Theta\left(e^{-\gamma h^{1+q} - q \log(h)}\right) \quad \text{as } h \uparrow \infty.$$

It is no surprise that Theorem 2.4 is comparable to Theorem 2.2, since setting $L = 1$ equates the Langevin and Hamiltonian methods.

2.2 The small h regime

It is straightforward to see that as $h \downarrow 0$ the random walk, Langevin and Hamiltonian candidate kernels will essentially behave equivalently in the first coordinate. Indeed, the Euclidean distance between the first coordinates of the random walk and Langevin proposals for any fixed $x \in \mathbb{R}^d$ is $h^2 |\partial \log \pi(x) / \partial x_1|$, while the random walk proposal displacement is $\Theta(h)$. The following result makes this intuition precise.

Proposition 2.2. *The Total Variation distance between the (Gaussian) random walk and Langevin proposals, each with scale $h > 0$, for a fixed $x \in \mathbb{R}$, denoted $Q_h^R(x, \cdot)$ and $Q_h^M(x, \cdot)$ respectively, is*

$$\|Q_h^M(x, \cdot) - Q_h^R(x, \cdot)\|_{TV} = 2\Phi^*\left(\frac{h}{4} |\nabla \log \pi(x)|\right) - 1,$$

where $\sqrt{2\pi}\Phi^*(z) := \int_{-\infty}^z e^{-u^2/2} du$.

The same intuition applies to the Hamiltonian case provided L is fixed, since each gradient term in the proposal is also $\Theta(h^2)$. While there are many well-known measures of distance between two distributions, we argue that total variation is an appropriate choice here, since it has an explicit focus on how much the two kernels overlap. Note that as $h \downarrow 0$ both $Q_h^R(x, \cdot)$ and $Q_h^M(x, \cdot)$ converge weakly to $\delta_x(\cdot)$, a Dirac measure centred at x , but that for any positive h it holds that $\|Q_h^R(x, \cdot) - \delta_x(\cdot)\|_{TV} = \|Q_h^M(x, \cdot) - \delta_x(\cdot)\|_{TV} = 1$.

While the above statements provide useful heuristic arguments, in order to obtain more rigorous results one should prove that the spectral gaps of the random walk Metropolis, MALA and HMC decay to 0 at the same rate as $h \downarrow 0$. The conjecture that the algorithms being similarly for small values of h is supported by the simulations of Section 5.1.

2.3 Extensions

There are a few natural ways to extend or alter the framework. One is to consider reducing the scale of the first k components to λ , rather than only the first. In fact, the lower bound of Theorem 2.1 extends to this scenario, becoming instead $\geq \Theta(h^{-k})$, and so the rate of decay remains polynomial in h for any k . Analogously, we expect the corresponding upper bound for gradient-based schemes to remain exponential and become $\leq \Theta\left(e^{-k(\gamma h^{1+q} - q \log(h))}\right)$, although the details of this are left for future work. We explore examples of this nature through simulations in Section 5 and find empirically that the single component case is informative also of more general cases.

Another natural way to consider the degree of heterogeneity of a distribution is to view the scales as samples from some probability distribution, which itself has a global scale parameter, and then increase this. In fact, this approach was taken in Roberts and Rosenthal [2001], in which the target was chosen as $\pi(x) = \prod_{i=1}^d C_i f(C_i x_i)$ with each C_i samples from a distribution with $\mathbb{E}[C_i^2] = b < \infty$. The asymptotic regime in that work is distinctly different to that presented here, however, since the degree of heterogeneity b is fixed and the $d \rightarrow \infty$ regime is considered. Nonetheless, the authors show that also in this limit the performance of MALA is more sensitive to tuning than the random walk algorithm, corroborating the results of the present article. See also Beskos et al. [2018] for a related work.

3 Combining robustness and efficiency

The results of Section 2 show that the two gradient-based samplers are much less robust to heterogeneity than the random walk algorithm. In this section, we introduce a novel and simple to implement gradient-based scheme that shares the superior scaling properties of the Langevin and Hamiltonian schemes, but also retains the robustness of the random walk sampler, both in terms of geometric ergodicity and robustness to heterogeneity.

3.1 Locally-balanced Metropolis–Hastings

In the ‘locally-balanced’ framework for Metropolis–Hastings, first introduced in Zanella [2019] for discrete state spaces, candidate kernels are of the form

$$\tilde{Q}(x, dy) = \tilde{Z}(x)^{-1} g\left(\frac{\pi(y)}{\pi(x)}\right) \mu_\sigma(y - x) dy, \quad (3.1)$$

where $g : (0, \infty) \rightarrow (0, \infty)$ is called a *balancing function*, and $\tilde{Z}(x) := \int g(\pi(y)/\pi(x)) \mu_\sigma(y - x) dy$. The kernel $\mu_\sigma(y - x) := \sigma^{-d} \mu((y - x)/\sigma)$ for some symmetric density μ serves to ensure the proposals are ‘local’ to the current point x , while the ratio $\pi(y)/\pi(x)$ gives more weight to points that have a higher density than x . The motivation for the balancing function g is to control for the fact that the weighting $\pi(y)/\pi(x)$ will not be optimal when combined with μ_σ . See Zanella [2019] for more discussion on this point and theoretical results suggesting that functions g satisfying $g(t) = tg(1/t)$ lead to asymptotically optimal Metropolis–Hastings proposals in (3.1).

In this paper we consider gradient-based versions of (3.1) based on a first-order Taylor series expansion of $\log \pi$, leading to the family of proposal distributions

$$Q(x, dy) = Z(x)^{-1} g\left(e^{\nabla \log \pi(x)(y-x)}\right) \mu_\sigma(y - x) dy, \quad (3.2)$$

where $Z(x) := \int g(e^{\nabla \log \pi(x)(y-x)}) \mu_\sigma(y - x) dy$. Remarkably, if the balancing function $g(t) = \sqrt{t}$ and a Gaussian kernel μ_σ are chosen, then the result is the Metropolis-adjusted Langevin algorithm

$$Q^M(x, dy) \propto e^{\nabla \log \pi(x)^T (y-x)/2} \mu_\sigma(y - x) dy.$$

Thus, the Langevin algorithm can be viewed as a particular instance of this class. Other choices of g are, however, also possible, and give rise to different gradient-based algorithms. In the next section we explore what a sensible choice of g might look like.

3.2 First-order exact methods

Intuitively, we would like any method that uses gradient information to be exact at the first order. In a Metropolis–Hastings context, this means a proposal that incorporates gradient information should be reversible with respect to measures that possess a log-linear density function, i.e. $\pi(x) = \exp(a^T x + b)$ for some $a \in \mathbb{R}^d$ and $b \in \mathbb{R}$. In such cases the gradient at any location encompasses full information and this would therefore seem to be a sensible minimal goal for well-designed gradient-based methods. The Langevin and Hamiltonian schemes both satisfy this stipulation. As the following proposition shows, for any instance of the class defined in (3.2), the condition $g(t) = tg(1/t)$ is both sufficient and necessary for the proposal distribution to satisfy such a requirement.

Proposition 3.1. *Let μ_σ be symmetric and $\pi(x) = \exp(a^T x + b)$ for some $a \in \mathbb{R}^d$ and $b \in \mathbb{R}$, with $a \neq 0$. Then a transition kernel of the form in (3.2) is π -reversible if and only if $g(t) = tg(1/t)$ for every $t > 0$.*

Remark 3.1. Note that $\pi(x) = \exp(a^T x + b)$ is an improper density function because $\int_{\mathbb{R}^d} \exp(a^T x + b) dx = \infty$ for any choice of a and b . This, however, does not pose any issue in defining π -reversible kernels as usual.

The special case $g(t) = \sqrt{t}$ adheres to Proposition 3.1, as $tg(1/t) = t/\sqrt{t} = \sqrt{t}$, but there are clearly many other admissible choices. A challenge in the general state space setting is to choose g in such a way that both $g(t) = tg(1/t)$, and that $Z(x)$ is tractable in (3.2). This is possible in the square root case provided μ_σ is a Gaussian kernel, and next we consider a different choice for which this can also be done.

3.3 The Barker proposal on \mathbb{R}

The requirement for the balancing function g to satisfy $g(t) = tg(1/t)$ is in fact the same condition imposed on the acceptance rate of a Metropolis–Hastings algorithm to produce a π -reversible Markov chain. Indeed, setting $t := \pi(y)q(y, x)/(\pi(x)q(x, y))$ and assuming $\alpha(x, y) := \alpha(t)$, then the detailed balance equations can precisely be written $\alpha(t) = t\alpha(1/t)$. Possible choices of g can therefore be found by considering suggestions for α in the literature. One choice proposed in Barker [1965] is

$$g(t) = \frac{t}{1+t}.$$

In the context of acceptance rates, this leads to the ‘Barker rule’ $\alpha(x, y) = \pi(y)q(y, x)/(\pi(x)q(x, y) + \pi(y)q(y, x))$. The work of Peskun [1973] and Tierney [1998] showed that this choice of α is inferior to the more familiar Metropolis–Hasting rule $\alpha(t) = \min(1, t)$ in terms of asymptotic variance. The same conclusion cannot, however, be drawn when considering the choice of balancing function g .

In fact, the choice $g(t) = t/(1+t)$ was shown to minimize asymptotic variances of Markov chain estimators in some discrete settings in Zanella [2019]. In addition, as shown below, this particular choice of g leads to a fully tractable candidate kernel that can be easily sampled from.

Proposition 3.2. *If $g(t) = t/(1+t)$, then the normalising constant $Z(x)$ in (3.2) is $1/2$.*

The resulting proposal distribution is

$$Q^B(x, dy) = 2 \frac{\mu_\sigma(y - x)}{1 + e^{-\nabla \log \pi(x)(y-x)}} dy. \quad (3.3)$$

We refer to Q^B as the *Barker proposal*. A simple sampling strategy to generate $y \sim Q^B(x, \cdot)$ is given below.

Algorithm 1 Generating a Barker proposal on \mathbb{R}

Require: the current point $x \in \mathbb{R}$.

1. Draw $z \sim \mu_\sigma(\cdot)$
2. Calculate $p(x, z) = 1/(1 + e^{-z \nabla \log \pi(x)})$
3. Set $b(x, z) = 1$ with probability $p(x, z)$, and $b(x, z) = -1$ otherwise
4. Set $y = x + b(x, z) \times z$

Output: the resulting proposal y .

Proposition 3.3. *Algorithm 1 produces a sample from Q^B on \mathbb{R} .*

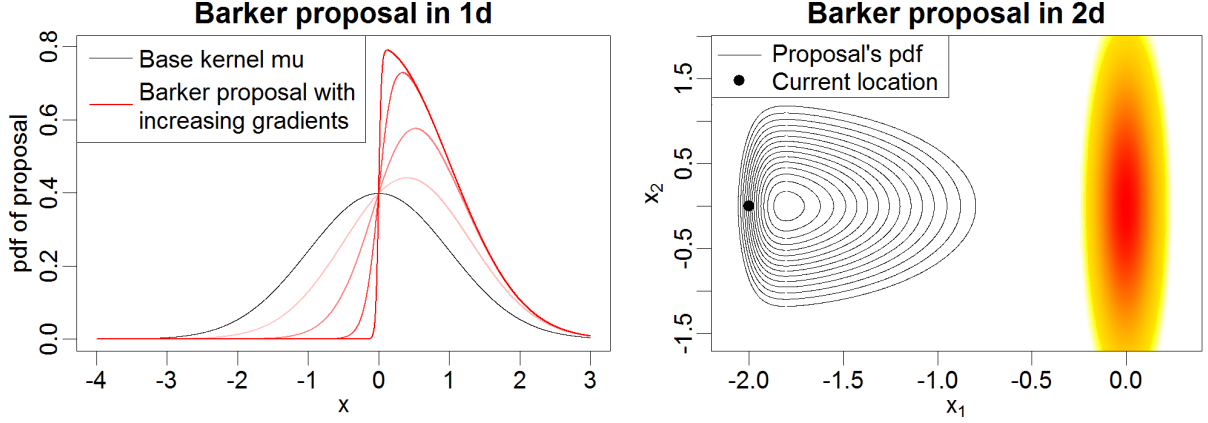


Figure 1: Left: density of the Barker proposal in one dimension. Current location is $x = 0$ and the four lines with increasing red intensity correspond to $\nabla \log \pi(x)$ equal to 1, 3, 10 and 50. Right: density of the Barker proposal in two dimensions. Solid lines display the proposal density contours, heat colours refer to the target density, and the current location is $x = (-2, 0)$.

Algorithm 1 shows that the magnitude $|y - x| = |z|$ of the proposed move does not depend on the gradient $\nabla \log \pi(x)$ here, it is instead dictated only by the choice of symmetric kernel μ_σ . The *direction* of the proposed move is, however, informed by the gradient. Examining the form of $p(x, z)$, it becomes clear that if the signs of z and $\nabla \log \pi(x)$ are in agreement, then $p(x, z) > 1/2$, and indeed as $z \nabla \log \pi(x) \uparrow \infty$ then $e^{-z \nabla \log \pi(x)} \downarrow 0$ and so $p(x, z) \uparrow 1$. Hence, if the indications from $\nabla \log \pi(x)$ are that $\pi(x + z) \gg \pi(x)$, then it is highly likely that $b(x, z)$ will be set to 1 and $y = x + z$ will be the proposed move. Conversely, if $z \nabla \log \pi(x) < 0$, then there is a larger than 50% chance that the proposal will instead be $y = x - z$. As $\nabla \log \pi(x) \uparrow \infty$ the Barker proposal converges to μ_σ truncated on the right, and similarly to μ_σ truncated on the left as $\nabla \log \pi(x) \downarrow -\infty$. See Figure 1 for an illustration.

The multiplicative term $1/(1 + e^{-\nabla \log \pi(x)(y-x)})$ in (3.3), which incorporates the gradient information, injects skewness into the base kernel μ_σ (as can be clearly seen in the left-hand plot of Figure 1). Indeed, the resulting distribution Q^B is an example of a *skew-symmetric* distribution [Azzalini, 2013, eq.(1.3)]. Skew-symmetric distributions are a tractable family of (skewed) probability density functions that are obtained by multiplying a symmetric base density function with the cumulative distribution function (cdf) of a symmetric random variable. We refer to Azzalini [2013, Ch.1] for more details, including a more general version of Propositions 3.2 and 3.3. In the context of skewed distributions the Gaussian cdf is often used, leading to the skew-normal distribution introduced in Azzalini [1985]. In our context, however, the Barker proposal (which leads to the logistic cdf $p(x, z)$ in Algorithm 1) is the only skew-symmetric distribution that can be obtained from (3.2) using a balancing function g satisfying $g(t) = tg(1/t)$. See the supplement for more detail.

3.4 The Barker proposal on \mathbb{R}^d

There are two natural ways to extend the Barker proposal to \mathbb{R}^d , for $d > 1$. The first is to treat each coordinate separately, and generate the proposal $y = (y_1, \dots, y_d)$ by applying Algorithm 1 independently to each coordinate. This corresponds to generating a z_i and $b_i(x, z_i)$ for each $i \in \{1, \dots, d\}$, and choosing the sign of each b_i using

$$p_i(x, z_i) = \frac{1}{1 + e^{-z_i \partial_i \log \pi(x)}},$$

where $\partial_i \log \pi(x)$ denotes the partial derivative of $\log \pi(x)$ with respect to x_i . Writing $Q_i^B(x, dy_i)$ to denote the resulting Barker proposal candidate kernel for the i th coordinate, for full candidate kernel Q^B can then be written

$$Q^B(x, dy) = \prod_{i=1}^d Q_i^B(x, dy_i). \quad (3.4)$$

The full Metropolis–Hastings scheme using the Barker proposal mechanism for a target distribution is given in Algorithm 2 (see also Section E of the supplement for more details and variations of the algorithm, such as preconditioning). Note that the computational cost of each iteration of the algorithm is basically equivalent to the one of MALA and will be typically dominated by the cost of computing the gradient and density of the target.

Algorithm 2 Metropolis–Hastings with the Barker proposal on \mathbb{R}^d

Require: starting point for the chain $x^{(0)} \in \mathbb{R}$, and scale $\sigma > 0$.

Set $t = 0$ and do the following:

1. Given $x^{(t)} = x$, draw y_i using Algorithm 1 independently for $i \in \{1, \dots, d\}$
2. Set $x^{(t+1)} = y$ with probability $\alpha^B(x, y)$, where

$$\alpha^B(x, y) = \min \left(1, \frac{\pi(y)}{\pi(x)} \times \prod_i \frac{1 + e^{(x_i - y_i) \partial_i \log \pi(x)}}{1 + e^{(y_i - x_i) \partial_i \log \pi(y)}} \right). \quad (3.5)$$

Otherwise set $x^{(t+1)} = x$

3. If $i + 1 < N$, set $i \leftarrow i + 1$ and return to step 1, otherwise stop.

Output: the Markov chain $\{x^{(0)}, \dots, x^{(N)}\}$.

The second approach is to apply the Barker scheme directly in the multidimensional setting. This consists of sampling $z \in \mathbb{R}^d$ from a d -dimensional symmetric distribution, and then choosing whether or not to flip the sign of *every* coordinate at the same time, using a single global $\tilde{b}(x, z) \in \{-1, 1\}$, to produce the global proposal $y = x + \tilde{b}(x, z) \times z$. In this case the probability that $\tilde{b}(x, z) = 1$ will be

$$\tilde{p}(x, z) = \frac{1}{1 + e^{-z^T \nabla \log \pi(x)}}. \quad (3.6)$$

This second approach doesn't allow gradient information to feed into the proposal as effectively as in the first case. Specifically, only the global inner product $z^T \nabla \log \pi(x)$ is considered, and the decision to alter the sign of every component of z is taken based solely on this value. Indeed, the following proposition shows that this strategy cannot improve over the random walk Metropolis by more than a factor of two.

Proposition 3.4. *Let \tilde{P}^B denote the modified Barker proposal on \mathbb{R}^d using (3.6). Then $\text{Gap}(P^R) \geq \text{Gap}(\tilde{P}^B)/2$.*

One can also make a stronger statement than the above proposition, namely that if this strategy is employed, only a constant factor improvement over the Random Walk Metropolis can be achieved in terms of asymptotic variance, for any $L^2(\pi)$ function of interest. Given Proposition 3.4 one should clearly prefer to use the first strategy described to produce Barker proposals on \mathbb{R}^d , and the multi-dimensional candidate kernel given in (3.4). In the following sections we will show both theoretically and empirically that our recommended version does indeed have favourable robustness and efficiency properties.

4 Robustness, scaling and ergodicity results for the Barker proposal

In this section we establish results concerning robustness to heterogeneity, scaling with dimension and geometric ergodicity for the Barker proposal scheme. As we will see, the latter enjoys the superior efficiency of gradient-based algorithms in terms of scaling with dimension, but also shares the favourable robustness properties of the random walk Metropolis when considering both robustness to heterogeneity and geometric ergodicity.

4.1 Robustness to heterogeneity

We now examine the robustness to heterogeneity of the Barker proposal using the framework introduced in Section 2. We therefore consider a Barker proposal on \mathbb{R}^d in which the first coordinate has step-size $h\sigma > 0$, and all other coordinates have step-sizes equal to σ . We denote the resulting proposal distribution Q_h^B and the corresponding Metropolis–Hastings transition kernel by P_h^B . From (3.3) and (3.4) it follows that the density function of Q_h^B is

$$q_h^B(x, y) = 2^d \frac{\mu_{\sigma h}(y_1 - x_1) \prod_{i=2}^d \mu_{\sigma}(y_i - x_i)}{\prod_{i=1}^d (1 + e^{-\partial_i \log \pi(x)(y_i - x_i)})}. \quad (4.1)$$

We write P^B to denote the case $h = 1$.

The following result characterizes the behavior of the spectral gap of P_h^B as $h \uparrow \infty$.

Theorem 4.1. *Assume Condition 2.1 and $\text{Gap}(P^B) > 0$. Then it holds that*

$$\text{Gap}(P_h^B) = \Theta(h^{-1}), \quad \text{as } h \uparrow \infty.$$

Comparing Theorem 4.1 with Theorems 2.1-2.4 from Section 2.1 we see that the Barker proposal inherits the robustness to heterogeneity of random walk schemes and is significantly more robust than MALA and HMC. In the next section we establish general conditions under which $\text{Gap}(P^B) > 0$.

4.2 Geometric ergodicity

In this section we study the class of target distributions for which the Barker proposal produces a geometrically ergodic Markov chain. We show that geometric ergodicity can be obtained even when the gradient term in the proposal grows faster than linearly, which is typically not the case for MALA and HMC.

We prove geometric ergodicity results for generic proposals as in (3.2), assuming g to be bounded and monotone, and μ_{σ} to have lighter than exponential tails. Following the discussion in Section 3.4 we consider proposals that are independent across components, leading to

$$Q^{(g)}(x, dy) = \prod_{i=1}^d Q_i^{(g)}(x, dy_i) = \prod_{i=1}^d \frac{g(e^{\partial_i \log \pi(x)(y_i - x_i)}) \mu_{\sigma}(y_i - x_i) dy_i}{Z_i(x)}, \quad (4.2)$$

where $Z_i(x) := \int_{\mathbb{R}} g(e^{\partial_i \log \pi(x)(y_i - x_i)}) \mu_{\sigma}(y_i - x_i) dy_i$. With a slight abuse of notation, we use μ_{σ} to represent one and d -dimensional densities. The Barker proposal in (3.4) is the special case obtained by taking $g(t) = t/(1+t)$.

For the results of this section, we make the simplifying assumption that π is spherically symmetric outside a ball of radius $R < \infty$.

Condition 4.1. *There exists $R < \infty$ and a differentiable function $f : (0, \infty) \rightarrow (0, \infty)$ with $\lim_{r \rightarrow \infty} f'(r) = -\infty$ and $f'(r)$ non-increasing for $r > R$ such that $\log \pi(x) = f(\|x\|)$ for $r > R$.*

Theorem 4.2. *Let $g : (0, \infty) \rightarrow (0, \infty)$ be a bounded and non-decreasing function, $\int_{\mathbb{R}} \exp(sw) \mu_{\sigma}(w) dw < \infty$ for every $s > 0$, and $\inf_{w \in (-\delta, \delta)} \mu_{\sigma}(w) > 0$ for some $\delta > 0$. If the target density π satisfies Condition 4.1, then the MH chain with proposal $Q^{(g)}$ is π -a.e. geometrically ergodic.*

We note that tail regularity assumptions such as Condition 4.1 are common in this type of analysis (e.g. Jarner and Hansen [2000], Durmus et al. [2017a]). As an intuitive example, the condition is satisfied in the exponential family $\pi(x) \propto \exp(-\alpha \|x\|^{\beta})$ for all $\beta > 1$. As a contrast, for MALA and HMC it is known that for $\beta > 2$ the sampler fails to be geometrically ergodic [Roberts and Tweedie, 1996, Livingstone et al., 2019]. We expect the Barker proposal to be geometrically ergodic also for the case $\beta = 1$, although we do not prove it in this work.

4.3 Scaling with dimensionality

In this section we provide preliminary results suggesting that the Barker proposal enjoys scaling behaviour analogous to that of MALA in high-dimensional settings, meaning that under appropriate assumptions it requires the number of iterations per effective sample to grow as $\Theta(d^{1/3})$ with the number of dimensions d as $d \rightarrow \infty$. Similarly to Section 4.2, we prove results for general proposals $Q^{(g)}$ as in (4.2) with balancing functions g satisfying $g(t) = t g(1/t)$. The Barker proposal is a special case of the latter family.

We perform an asymptotic analysis for $d \rightarrow \infty$ using the framework introduced in Roberts et al. [1997]. The main idea is to study the rate at which the proposal step size σ needs to decrease as $d \rightarrow \infty$ to obtain well-behaved limiting behaviour for the MCMC algorithm under consideration (such as a $\Theta(1)$ acceptance rate and convergence to a non-trivial diffusion process after appropriate time re-scaling). Based on the rate of decrease of σ one can infer how the number of MCMC iterations required for each effective sample increases as $d \rightarrow \infty$. For example, in the case of the random walk Metropolis σ^2 must be scaled as $\Theta(d^{-1})$ as $d \rightarrow \infty$ to have a well-behaved limit [Roberts et al., 1997], which leads to RWM requiring $\Theta(d)$ iterations for each effective sample. By contrast, for MALA it is sufficient to take $\sigma^2 = \Theta(d^{-1/3})$ as $d \rightarrow \infty$, which leads to only $\Theta(d^{1/3})$ iterations for each effective sample [Roberts and Rosenthal, 1998]. While these analyses are typically performed under simplifying assumptions, such as having a target distribution with i.i.d. components, the results have been extended in many ways (e.g. removing the product-form assumption, see Mattingly et al. [2012]) obtaining analogous conclusions. See also Beskos et al. [2013] for optimal scaling analysis of HMC and Roberts and Rosenthal [2016] for rigorous connections between optimal scaling results and computational complexity statements.

In this section we focus on the scaling behaviour of Metropolis–Hastings algorithms with proposal $Q^{(g)}$ as in (4.2), when targeting distributions of the form $\pi(x) = \prod_{i=1}^d f(x_i)$, where f is a one-dimensional smooth density function. Given the structure of $Q^{(g)}$ and $\pi(\cdot)$, the acceptance rate takes the form $\alpha(x, y) = \min \left\{ 1, \prod_{i=1}^d \alpha_i(x_i, y_i) \right\}$, where

$$\alpha_i(x_i, y_i) = \frac{f(y_i)}{f(x_i)} \frac{g \left(e^{\phi'(y_i)(x_i - y_i)} \right)}{g \left(e^{\phi'(x_i)(y_i - x_i)} \right)} \frac{Z_i(x_i)}{Z_i(y_i)}, \quad (4.3)$$

and $\phi = \log f$. In such a context, the scaling properties of the MCMC algorithms under consideration are typically governed by the behaviour of $\log(\alpha_i(x_i, y_i))$ as y_i gets close to x_i , or more precisely by degree of the leading term in the Taylor expansion of $\log(\alpha_i(x_i, x_i + \sigma u_i))$ in powers of σ as $\sigma \rightarrow 0$ for fixed x_i and u_i . For example, in the case of the random walk Metropolis one has $\log(\alpha_i(x_i, x_i + \sigma u_i)) = \Theta(\sigma)$ as $\sigma \rightarrow 0$, which in fact implies the proposal variance σ^2 must decrease at a rate $\Theta(d^{-1})$ to obtain a non-trivial limit. By contrast, when the MALA proposal is used, one has $\log(\alpha_i(x_i, x_i + \sigma u_i)) = \Theta(\sigma^3)$ as $\sigma \rightarrow 0$, which in turn leads to $\sigma^2 = \Theta(d^{-1/3})$. See Sections 2.1–2.2 of Durmus et al. [2017b] for a more detailed and rigorous discussion on the connection between the Taylor expansion of $\log(\alpha_i(x_i, y_i))$ and

MCMC scaling results. The following proposition shows that the condition $g(t) = tg(1/t)$, when combined with some smoothness assumptions, is sufficient to ensure that the proposals $Q^{(g)}$ lead to $\log(\alpha_i(x_i, x_i + \sigma u_i)) \leq \Theta(\sigma^3)$ as $\sigma \rightarrow 0$.

Proposition 4.1. *Let $g : (0, \infty) \rightarrow (0, \infty)$ and $g(t) = tg(1/t)$ for all t . If g is three times continuously differentiable and $\int_{\mathbb{R}} g(\exp(sw))\mu(w)dw < \infty$ for all $s > 0$ and $j \in \{0, 1, 2, 3\}$, where $g^{(j)} : (0, \infty) \rightarrow (0, \infty)$ is the j -th derivative of g , then*

$$\log(\alpha_i(x_i, x_i + \sigma u_i)) \leq \Theta(\sigma^3) \quad \text{as } \sigma \rightarrow 0, \quad (4.4)$$

for any x_i and u_i in \mathbb{R} .

Proposition 4.1 suggests that Metropolis–Hastings algorithms with proposals $Q^{(g)}$ such that $g(t) = tg(1/t)$ have scaling behaviour analogous to MALA, meaning that $\sigma^2 = \Theta(d^{-1/3})$ is sufficient to ensure a non-trivial limit and thus $\Theta(d^{1/3})$ iterations are required for each effective sample. To make these arguments rigorous one should prove weak convergence results for $d \rightarrow \infty$, as in Roberts and Rosenthal [1998]. Proving such a result for a general g would require a significant amount of technical work, thus going beyond the scope of this section. In this paper we rather support the conjecture of $\Theta(d^{1/3})$ scaling for $Q^{(g)}$ by means of simulations (see Section 5.2). While Proposition 4.1 only shows $\log(\alpha_i(x_i, x_i + \sigma u_i)) \leq \Theta(\sigma^3)$, it is possible to show that $\log(\alpha_i(x_i, x_i + \sigma u_i)) = \Theta(\sigma^3)$ with some extra assumptions on ϕ to exclude exceptional cases (see Remark B.1 in the supplement).

5 Simulations

Throughout this section we choose the symmetric density μ_σ within the random walk and Barker proposal to be that of a $N(0, \sigma^2)$ distribution for simplicity. Note, however, that alternatives are possible.

5.1 Illustrations of robustness to heterogeneity

We first provide a simple illustration of the robustness to heterogeneity of the random walk (RW), Langevin and Barker algorithms in three simple one-dimensional settings. In each case we approximate the expected squared jump distance using 10^4 Monte Carlo samples and standard Rao–Blackwellisation techniques, across of range of different proposal step-sizes between 0.01 and 100. As is clearly shown in Figure 2, all algorithms perform similarly when the step-size is smaller than optimal, as suggested in Section 2.2. As the step-size increases beyond this optimum, however, behaviours begin to differ. In particular the expected squared jump distance for MALA rapidly decays to zero, whereas in the random walk and Barker cases the reduction is much less pronounced. In fact, the rate of decay is similar for the two schemes, which is to be expected following the results of Sections 4.1 and 2.1. See also Figure 8 in the supplement for a similar illustration on a 20-dimensional example.

5.2 Comparison of efficiency on isotropic targets

Next we compare the expected squared jump distance of the random walk, Langevin and Barker schemes when sampling from isotropic Gaussian distributions of increasing dimension, with optimised proposal scale (chosen to maximise expected squared jumping distance). This setup is favourable to MALA, which is the less robust scheme among the one under comparison, as the target distribution is homogeneous and the proposal step-size well-chosen. Figure 3 shows how the expected squared jump distance (ESJD) per coordinate decays as dimension increases for the three algorithms. For MALA and the Barker scheme the ESJD appears to decrease at the same rate as d increases, which is in accordance with the preliminary results in Section 4.3.

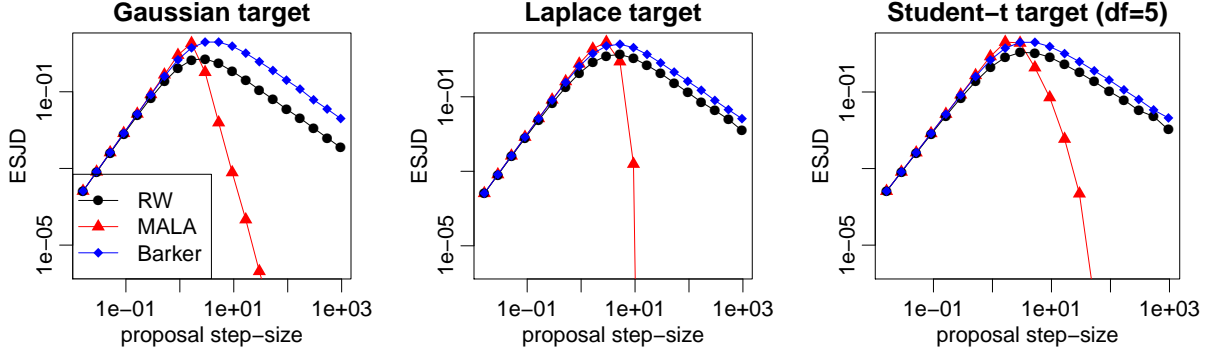


Figure 2: Expected squared jump distance (ESJD) against proposal step-size for RW, MALA and Barker on different 1-dimensional targets.

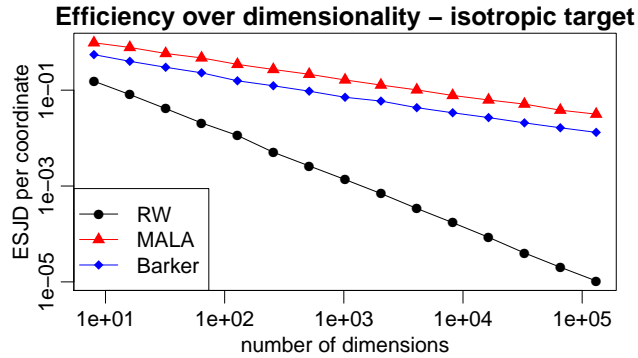


Figure 3: Expected squared jump distance (ESJD) against dimension for RW, MALA and Barker schemes.

Here MALA outperforms Barker roughly by a factor of 2 independently of dimensions (more precisely, for the simulations in Figure 3, the ratio lies between 1.7 and 2.5 for all values of d). The rate of decay for random walk is faster, as predicted by the theory.

5.3 Implications for Adaptive Markov chain Monte Carlo

In the remaining two examples we illustrate how robustness to heterogeneity affects the performance of adaptive MCMC methods. We consider adaptive versions of the random walk, Langevin and Barker schemes, using Algorithm 4 in Section 5 of Andrieu and Thoms [2008] for adaptation. Specifically, in each case a Markov chain is initialised using a chosen global proposal scale σ_0 and an identity pre-conditioning matrix $\Sigma_0 = I$ (a detailed description of how the Barker scheme was pre-conditioned is given in the supplement), and at each iteration the global scale and pre-conditioning matrix are updated using the equations

$$\log(\sigma_t) = \log(\sigma_{t-1}) + \gamma_t \times (\alpha(X_t, Y_t) - \bar{\alpha}_*) \quad (5.1)$$

$$\mu_t = \mu_{t-1} + \gamma_t \times (X_t - \mu_{t-1}) \quad (5.2)$$

$$\Sigma_t = \Sigma_{t-1} + \gamma_t \times ((X_t - \mu_t)(X_t - \mu_t)^T - \Sigma_{t-1}). \quad (5.3)$$

Here X_t denotes the current point in the Markov chain, Y_t is the proposed move, $\mu_0 = 0$ and $\bar{\alpha}_*$ denotes some ideal acceptance rate for the algorithm. The parameter γ_t is known as the learning rate. We set $\gamma_t := t^{-\kappa}$ as recommended in Shaby and Wells [2010]. In the first example Σ_t is constrained to be diagonal, and in Section 5.4 it is allowed to be dense (see the supplement for pseudo-code of the resulting algorithms). We set $\bar{\alpha}_*$ to be 0.23 for RW, 0.57 for MALA and

0.40 for Barker. We tried changing the value of $\bar{\alpha}_*$ for Barker in the range $[0.2, 0.6]$ without observing major differences.

Figure 4 shows the performance of the resulting algorithms when the distribution of interest $\pi(\cdot)$ is a 100-dimensional Gaussian with diagonal covariance matrix, in which the standard deviation of the first component is 0.01 and all other components have unit scale. Each sampler was initialised from the same random point obtained by sampling each coordinate independently from a $N(0, 10^2)$ distribution, and we set $\kappa = 0.6$.

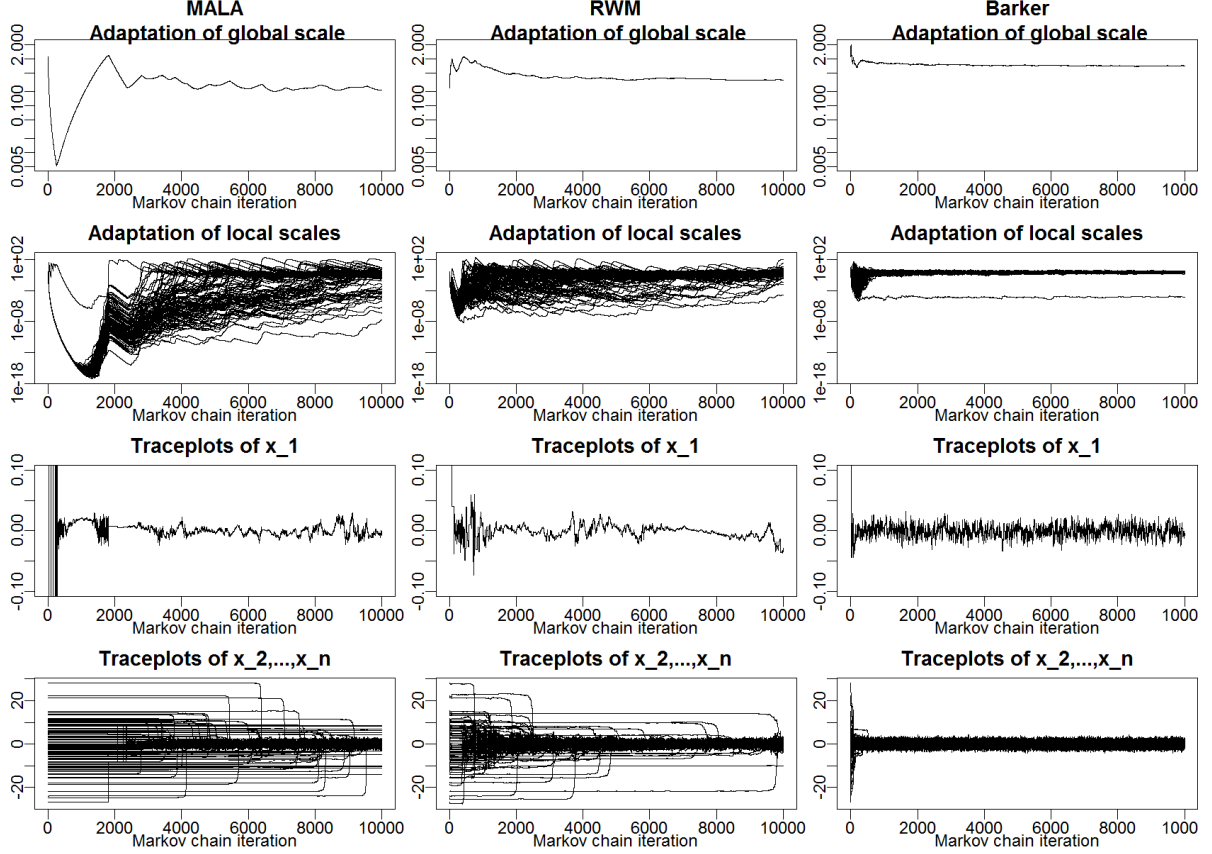


Figure 4: Comparison of adaptive versions of the RW, MALA and Barker schemes on a 100-dimensional target distribution in which the first component has standard deviation 0.01 and all others have unit scale. Both the adaptation parameters and the Markov chain trajectories are plotted. The learning rate is set to $\gamma_t = t^{-\kappa}$ with $\kappa = 0.6$.

We see a dramatic difference in behaviour among the three algorithms. For the Barker scheme adaptation stabilises within a few hundred iterations, after which algorithm performance appears to be stable and efficient. In order for MALA to achieve a non-zero acceptance rate the global scale parameter σ must first be reduced considerably to accommodate the smallest scale of $\pi(\cdot)$. At this point the algorithm can slowly begin to learn the components of the preconditioning matrix Σ , but this learning occurs very slowly because the comparatively small value for σ results in very slow mixing across all other dimensions than the first. The difference is that in the Barker scheme a much larger value for σ still results in a non-zero acceptance rate, which means that the local scales can be learned much more efficiently.

We performed the same experiment changing the learning rate's exponent to $\kappa = 0.4$ and $\kappa = 0.8$. The results are displayed in the supplement. The behaviour of RW and Barker was comparatively stable across all three different values of κ , while MALA was very sensitive to the choice of κ . The best performances for MALA are achieved in the case $\kappa = 0.4$, with smaller

values of κ leading to instability in the adaptation process. RW exhibits more stable behaviour than MALA, but still requires many iterations to learn reasonable adaptation parameters, and even after that it explores the posterior at a much slower rate than Barker.

The target considered above mirrors the theoretical framework of Sections 2 and 4.1 in the sense that a single coordinate is the source of heterogeneity. To move beyond this scenario, we consider a case in which the log-scales of each coordinate are sampled independently from a $N(0, \eta_{het}^2)$ distribution. In Figure 5 we consider $\eta_{het} = 1$ with $\kappa = 0.6$. We then increased

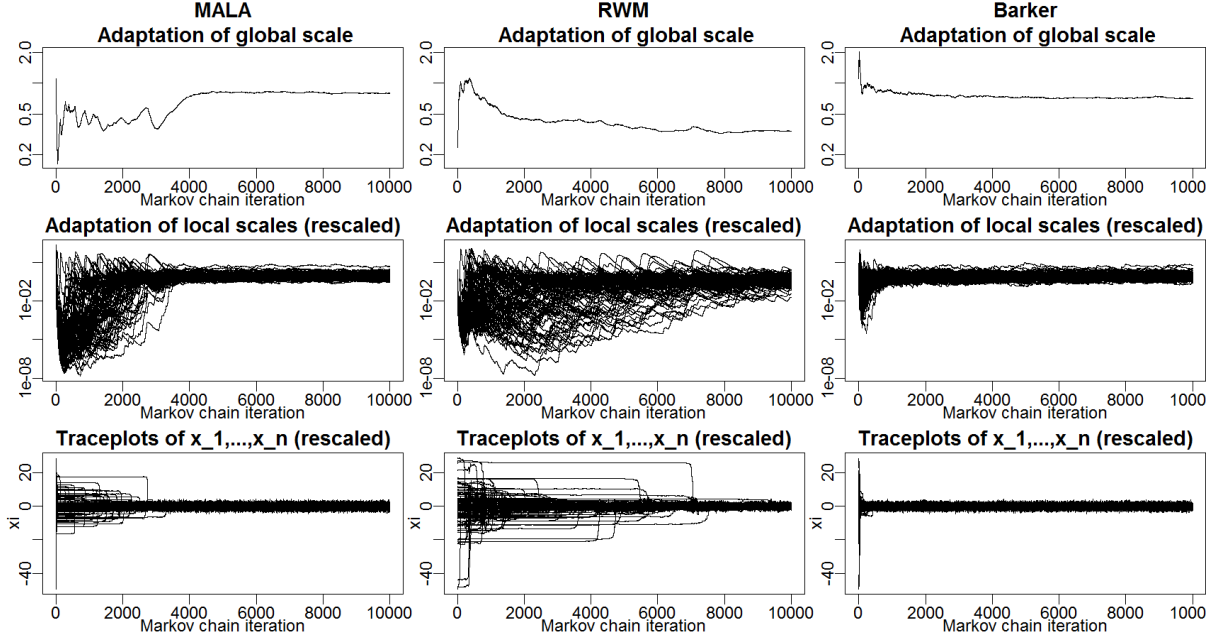


Figure 5: Comparison of adaptive versions of RW, MALA and Barker for a 100-dimensional target with $\log(\eta_i) \stackrel{iid}{\sim} N(0, \eta_{het}^2)$ with $\eta_{het} = 1$. In order to facilitate readability, in the plot we normalize the local scales $\Sigma_{t,ii}$ (see (5.3)) and the Markov chains components by the target standard deviation η_i . The adaptation learning rate was set to $\gamma_t = t^{-\kappa}$ with $\kappa = 0.6$.

the heterogeneity by setting $\eta_{het} = 3$. In this case the heterogeneity is more severe and MALA fails to converge in 10^4 steps for both $\kappa = 0.8$ (shown in supplement) and $\kappa = 0.6$ (shown in Figure 6), while the Barker scheme is stable in both cases. Lower values of κ led to instability for MALA.

5.4 Crossed random effects model example

Finally we consider the task of sampling from the posterior distribution of a Poisson random effects model of the form

$$y_{ij} \sim \text{Poisson}(\exp(\mu + a_i + b_j)) \quad (5.4)$$

for $i = 1, \dots, I$; $j = 1, \dots, J$ and prior distributions chosen to be $\mu \sim N(0, \sigma_\mu^2)$, each $a_i \sim N(0, \sigma_a^2)$ and each $b_j \sim N(0, \sigma_b^2)$. For our simulations we set $I = J = 50$, $\sigma_\mu = 10$, $\sigma_a = \sigma_b = 1$ and tested the algorithms on sampling from the posterior distribution $p(\mu, a, b|y)$, which in this case is a 101-dimensional distribution. The data y_{ij} were simulated from the model in (5.4) by setting $\mu = 1$ and sampling the values of a_i and b_j from their prior distributions.

Hierarchical models such as (5.4) are routinely used in Bayesian Statistics and can lead to strong posterior correlations, because of the weak identifiability of the parameters. In particular, the covariance matrix of the posterior distribution can have a large condition number and eigenvalues not aligned with the coordinates, representing a challenge for adaptive MCMC (see e.g.

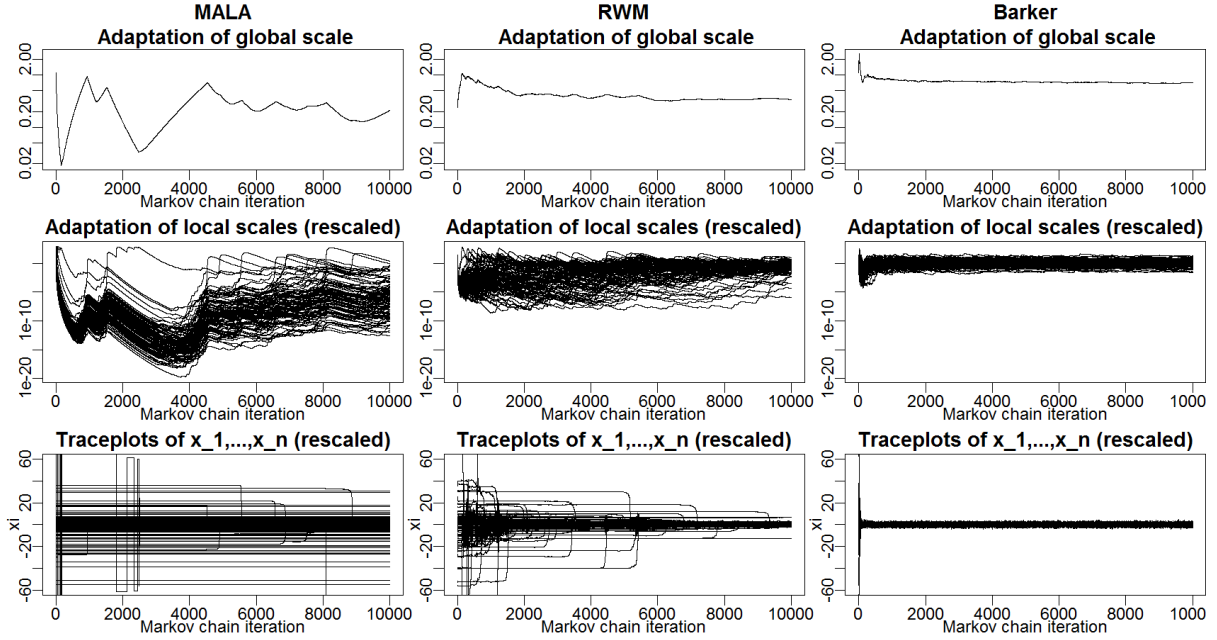


Figure 6: Comparison of adaptive versions of RW, MALA and Barker for a 100-dimensional target with $\log(\eta_i) \stackrel{iid}{\sim} N(0, \eta_{het}^2)$ with $\eta_{het} = 3$. Both the adaptation parameters and the Markov chains trajectories are plotted. The learning rate of the adaptation is set to $\gamma_t = t^{-\kappa}$ with $\kappa = 0.6$.

Zanella and Roberts [2019], Papaspiliopoulos et al. [2018] for more details). Here we consider versions of the algorithms in which a dense pre-conditioning matrix is adapted during sampling following (5.3) (in this example adapting only the diagonal results in poor performance). Figure 7 provides the results for $\kappa = 0.9$, and starting configuration with components sampled independently from a standard normal distribution. The random walk and Barker schemes converge to stationarity, with Barker the quickest, while MALA exhibits extremely poor mixing. We tried setting κ to lower values, namely 0.7 and 0.5, but the performance changed very little (details in the supplement). In these cases we also had to introduce some regularization in the covariance (namely pre-conditioning using $\Sigma_t + \epsilon I$ at each iteration rather than Σ_t , where $\epsilon = 10^{-5}$) to avoid instability in the adaptation process and degenerate covariances. In two further experiments, algorithms were first initialised from the posterior mode, and then additionally Σ_0 was chosen to be the inverted negative Hessian matrix of the log-posterior distribution evaluated at the mode. The results are shown in the supplement, and display behaviour comparable to Figure 7 in the MALA case, but some improvement for the random walk scheme.

As a sensitivity check, we also performed the same experiment using the tamed Metropolis-adjusted Langevin algorithm [Brosse et al., 2018] and the truncated Metropolis-adjusted Langevin algorithm [Roberts and Tweedie, 1996, Atchade, 2006], two more robust modifications to MALA in which large gradients are controlled by monitoring the size of $\|\nabla \log \pi(x)\|$. The schemes do offer some added stability compared to MALA in terms of controlling large gradients, but ultimately are still very sensitive to heterogeneity of the target distribution, and do not exhibit the same robustness observed in the case of the Barker scheme. See the supplement for implementation details, results and further discussion.

In order to show that the posterior distribution under consideration is non-trivial, we also attempted to fit the same model using the No-U-Turn Sampler variant of Hamiltonian Monte Carlo implemented in the Stan software [Carpenter et al., 2017], a state-of-the-art gradient-based MCMC implementation. Full details and results are provided in the supplement. The No-U-

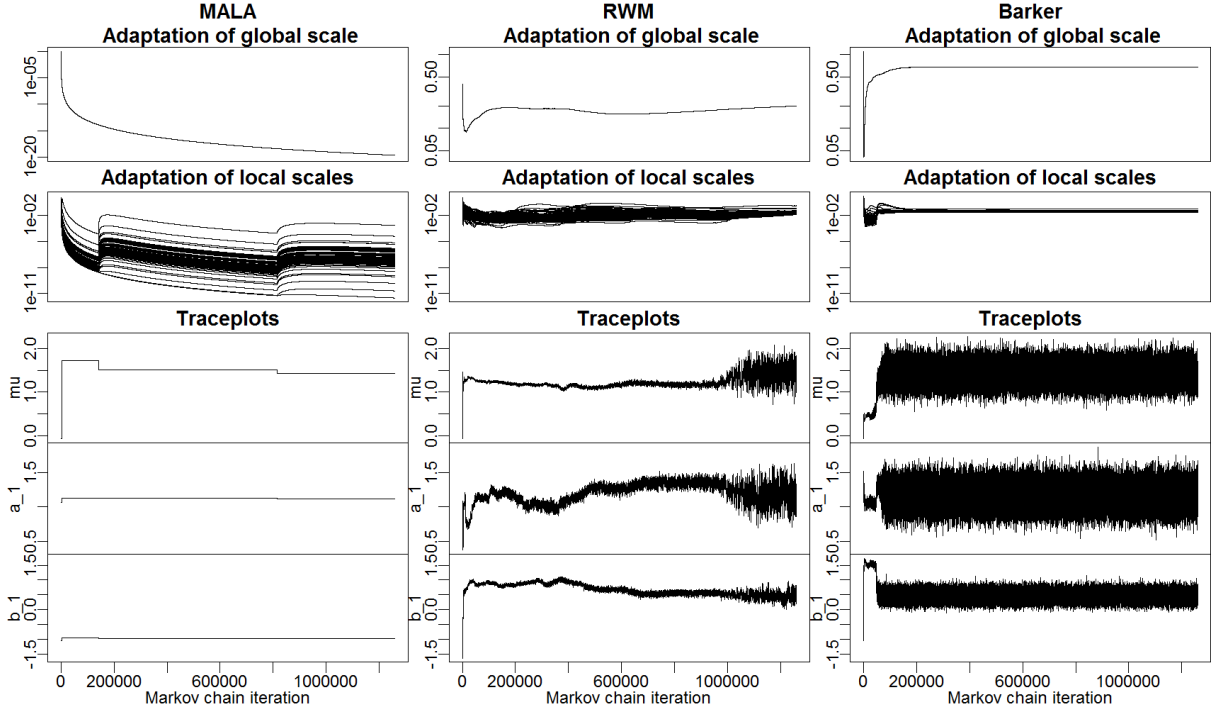


Figure 7: Comparison of RW, MALA and Barker on posterior distribution arising from a crossed random effect model with Poisson likelihood. Barker converges to stationarity faster than RW, while MALA fails to converge. Once in stationarity Barker mixes well (takes less than 20 iterations for each ESS) and outperforms RW in terms of ESJD and ESS by factors between 20 and 60.

Turn sampler with diagonal adaptive pre-conditioning manages to converge to stationarity, but achieves around three orders of magnitude fewer effective samples per gradient evaluation than the Barker scheme. When the setting are changed so that a dense pre-conditioning matrix is learned the No-U-Turn-Sampler fails to explore the target distribution and performs very poorly.

6 Discussion

We have provided a framework for characterising a new kind of robustness in Markov chain Monte Carlo, and used it to explore the relative merits of some popular Markov chain Monte Carlo methods, highlighting that commonly used schemes utilising gradients fail to be robust in this sense. We have also introduced a new algorithm, the Barker proposal scheme, which is both gradient-based and robust, as well as having desirable scaling and ergodicity properties. The most striking benefit of robustness to heterogeneity appears to be in the context of adaptive Markov chain Monte Carlo. Evidence suggests that combining the efficiency of a gradient-based proposal mechanism with a method that exhibits robustness to heterogeneity gives a combination of stability and speed that is very desirable in this setting, and can lead to efficient sampling that requires minimal practitioner input.

The theoretical results in this paper could be extended by studying in greater depth the small h regime (Section 2.2) and the high-dimensional scaling of the Barker scheme (Section 4.3). Of course, there are many other algorithms that could be considered under the heterogeneity framework introduced in this paper, and it is worthwhile future work to explore which features of a scheme result in either robustness to heterogeneity or a lack of it. Extensions to the Barker

scheme that incorporate momentum and exhibit the $d^{-1/4}$ decay in efficiency with dimension enjoyed by Hamiltonian Monte Carlo may be possible, as well as the development of other methods within the first-order locally-balanced proposal framework introduced in Section 3, or indeed schemes that are exact at higher orders.

Acknowledgements

The authors thank Marco Frangi for preliminary work in his Master’s thesis related to the ergodicity arguments in the paper. SL acknowledges support from the engineering and physical sciences research council through grant number EP/K014463/1 (i-like). GZ acknowledges support from the European research council starting grant 306406 (N-BNP), and by the Italian ministry of education, universities and research PRIN Project 2015SNS29B.

References

- Horst Alzer. On some inequalities for the incomplete gamma function. *Mathematics of Computation of the American Mathematical Society*, 66(218):771–778, 1997.
- Christophe Andrieu and Johannes Thoms. A tutorial on adaptive mcmc. *Statistics and computing*, 18(4):343–373, 2008.
- Yves F Atchade. An adaptive version for the metropolis adjusted langevin algorithm with a truncated drift. *Methodology and Computing in applied Probability*, 8(2):235–254, 2006.
- Adelchi Azzalini. A class of distributions which includes the normal ones. *Scandinavian journal of statistics*, pages 171–178, 1985.
- Adelchi Azzalini. *The skew-normal and related families*. Institute of Mathematical Statistics Monographs. Cambridge University Press, 2013.
- Av A Barker. Monte carlo calculations of the radial distribution functions for a proton-electron plasma. *Australian Journal of Physics*, 18(2):119–134, 1965.
- Alexandros Beskos, Natesh Pillai, Gareth Roberts, Jesus-Maria Sanz-Serna, and Andrew Stuart. Optimal tuning of the hybrid monte carlo algorithm. *Bernoulli*, 19(5A):1501–1534, 2013.
- Alexandros Beskos, Gareth Roberts, Alexandre Thiery, and Natesh Pillai. Asymptotic analysis of the random walk metropolis algorithm on ridged densities. *The Annals of Applied Probability*, 28(5):2966–3001, 2018.
- Steve Brooks, Andrew Gelman, Galin Jones, and Xiao-Li Meng. *Handbook of markov chain monte carlo*. CRC press, 2011.
- Nicolas Brosse, Alain Durmus, Éric Moulines, and Sotirios Sabanis. The tamed unadjusted langevin algorithm. *Stochastic Processes and their Applications*, 2018.
- Bob Carpenter, Andrew Gelman, Matthew D Hoffman, Daniel Lee, Ben Goodrich, Michael Betancourt, Marcus Brubaker, Jiqiang Guo, Peter Li, and Allen Riddell. Stan: A probabilistic programming language. *Journal of statistical software*, 76(1), 2017.
- Arnak S Dalalyan. Theoretical guarantees for approximate sampling from smooth and log-concave densities. *Journal of the Royal Statistical Society: Series B (Statistical Methodology)*, 79(3):651–676, 2017.

- Simon Duane, Anthony D Kennedy, Brian J Pendleton, and Duncan Roweth. Hybrid monte carlo. *Physics letters B*, 195(2):216–222, 1987.
- Alain Durmus and Eric Moulines. Nonasymptotic convergence analysis for the unadjusted langevin algorithm. *The Annals of Applied Probability*, 27(3):1551–1587, 2017.
- Alain Durmus, Eric Moulines, and Eero Saksman. On the convergence of hamiltonian monte carlo. *arXiv preprint arXiv:1705.00166*, 2017a.
- Alain Durmus, Gareth O Roberts, Gilles Vilmart, Konstantinos C Zygalakis, et al. Fast Langevin based algorithm for MCMC in high dimensions. *The Annals of Applied Probability*, 27(4):2195–2237, 2017b.
- Walter Gautschi. Some elementary inequalities relating to the gamma and incomplete gamma function. *Journal of Mathematics and Physics*, 38(1-4):77–81, 1959.
- W Keith Hastings. Monte carlo sampling methods using markov chains and their applications. 1970.
- Matthew D Hoffman and Andrew Gelman. The no-u-turn sampler: adaptively setting path lengths in hamiltonian monte carlo. *Journal of Machine Learning Research*, 15(1):1593–1623, 2014.
- Søren Fiig Jarner and Ernst Hansen. Geometric ergodicity of Metropolis algorithms. *Stochastic processes and their applications*, 85(2):341–361, 2000.
- Werner Krauth. *Statistical mechanics: algorithms and computations*, volume 13. OUP Oxford, 2006.
- Samuel Livingstone, Michael Betancourt, Simon Byrne, and Mark Girolami. On the geometric ergodicity of hamiltonian monte carlo. *Bernoulli*, page To appear, 2019.
- Jonathan C Mattingly, Natesh S Pillai, and Andrew M Stuart. Diffusion limits of the random walk Metropolis algorithm in high dimensions. *The Annals of Applied Probability*, 22(3): 881–930, 2012.
- Nicholas Metropolis, Arianna W Rosenbluth, Marshall N Rosenbluth, Augusta H Teller, and Edward Teller. Equation of state calculations by fast computing machines. *The journal of chemical physics*, 21(6):1087–1092, 1953.
- Radford M Neal. Slice sampling. *The annals of statistics*, 31(3):705–767, 2003.
- Radford M Neal. Mcmc using hamiltonian dynamics. *Handbook of markov chain monte carlo*, 2(11):2, 2011.
- Omiros Papaspiliopoulos, Gareth O Roberts, and Giacomo Zanella. Scalable inference for crossed random effects models. *arXiv preprint arXiv:1803.09460*, 2018.
- Peter H Peskun. Optimum monte-carlo sampling using markov chains. *Biometrika*, 60(3): 607–612, 1973.
- Gareth O Roberts and Jeffrey S Rosenthal. Optimal scaling of discrete approximations to Langevin diffusions. *Journal of the Royal Statistical Society: Series B (Statistical Methodology)*, 60(1):255–268, 1998.
- Gareth O Roberts and Jeffrey S Rosenthal. Optimal scaling for various Metropolis-Hastings algorithms. *Statistical science*, 16(4):351–367, 2001.

- Gareth O Roberts and Jeffrey S Rosenthal. General state space markov chains and mcmc algorithms. *Probability surveys*, 1:20–71, 2004.
- Gareth O Roberts and Jeffrey S Rosenthal. Complexity bounds for Markov chain Monte Carlo algorithms via diffusion limits. *Journal of Applied Probability*, 53(2):410–420, 2016.
- Gareth O Roberts and Richard L Tweedie. Exponential convergence of langevin distributions and their discrete approximations. *Bernoulli*, 2(4):341–363, 1996.
- Gareth O Roberts, Andrew Gelman, and Walter R Gilks. Weak convergence and optimal scaling of random walk Metropolis algorithms. *The annals of applied probability*, 7(1):110–120, 1997.
- Jeffrey S Rosenthal. Asymptotic Variance and Convergence Rates of Nearly-Periodic Markov Chain Monte Carlo Algorithms. *Journal of the American Statistical Association*, 98(461):169–177, 2003.
- Benjamin Shaby and Martin T Wells. Exploring an adaptive metropolis algorithm. *Technical report*, 2010.
- Andrew M Stuart. Inverse problems: a bayesian perspective. *Acta numerica*, 19:451–559, 2010.
- Luke Tierney. A note on metropolis-hastings kernels for general state spaces. *The Annals of Applied Probability*, 8(1):1–9, 1998.
- Dawn Woodard, Scott Schmidler, and Mark Huber. Sufficient conditions for torpid mixing of parallel and simulated tempering. *Electronic Journal of Probability*, 14:780–804, 2009.
- Giacomo Zanella. Informed proposals for local mcmc in discrete spaces. *Journal of the American Statistical Association*, pages 1–27, 2019.
- Giacomo Zanella and Gareth Roberts. Multilevel linear models, Gibbs samplers and multigrid decompositions. *arXiv preprint arXiv:1703.06098*, 2019.

Supplement to ‘On the robustness of gradient-based MCMC algorithms.’

The supplementary material contains proofs of the results, some background on the key techniques used for the proofs of Section 2, and establishes Condition 2.3 for the exponential family class. Additional figures related to the simulations and details related to skew-symmetry of the Barker proposal and pre-conditioning are also included.

A Tools to bound spectral gaps

To establish lower bounds on spectral gaps we use the following Lemma.

Lemma A.1. *Consider two Metropolis–Hastings kernels P_1 and P_2 with associated candidate kernels $Q_1(x, dy) = q_1(x, y)dy$ and $Q_2(x, dy) = q_2(x, y)dy$. If there is a $\gamma > 0$ such that $q_1(x, y) \geq \gamma q_2(x, y)$ for all fixed x, y with $x \neq y$, then*

$$\text{Gap}(P_1) \geq \gamma \text{Gap}(P_2). \quad (\text{A.1})$$

Proof. For any $f \in L^2_{0,1}(\pi)$, it holds that

$$\begin{aligned} \int \{f(y) - f(x)\}^2 \pi(dx) P_1(x, dy) &= \int \{f(y) - f(x)\}^2 \alpha(x, y) \pi(dx) Q_1(x, dy) \\ &\geq \gamma \int \{f(y) - f(x)\}^2 \alpha(x, y) \pi(dx) Q_2(x, dy) \\ &= \gamma \int \{f(y) - f(x)\}^2 \pi(dx) P_2(x, dy). \end{aligned}$$

The result follows from the Dirichlet forms characterization of spectral gaps in (2.2). \square

To find upper bounds we use the notion of *conductance* for a Markov chain. Define the conductance of a set $K \in \mathcal{B}$ with $0 < \pi(K) \leq 1/2$ for a π -reversible Markov chain with transition kernel P as

$$\Phi(K) := \frac{\int_K \pi(dx) P(x, K^c)}{\pi(K)},$$

which is the conditional probability $\mathbb{P}(X^{(t+1)} \in K^c | X^{(t)} \in K)$ provided $X^{(t)} \sim \pi(\cdot)$. Recall the spectral gap bound for P that for any such K

$$\text{Gap}(P) \leq 2\Phi(K). \quad (\text{A.2})$$

This can be seen directly by setting $g(x) = \pi(K^C)\mathbb{I}(x \in K) - \pi(K)\mathbb{I}(x \in K^c)$, letting $f(x) := g(x) / \int g(x)^2 \pi(dx)$ and computing the Dirichlet form of f using (2.2). Here $\mathbb{I}(\cdot)$ denotes the indicator function.

B Proofs

B.1 Proofs for Section 2

Proof of Proposition 2.1. We first establish that $\mu(\delta_h) \geq \mu(\delta)$ whenever $h \geq h_0$ for some $h_0 < \infty$. In cases (i) and (iii) $\mu(z)$ is monotonically decreasing in $\|z\|_2^2$. So when $h > 1$ it holds that

$$\|\delta_h\|_2^2 = \sum_{i=1}^d (y_i - x_i)^2 + h^{-2}(y_1 - x_1)^2 \leq \|\delta\|_2^2,$$

which proves the condition for $h_0 = 1$. In case (ii) $\mu(z)$ is monotonically decreasing in $\|z\|_1$, so again $\|\delta_h\|_1 = h^{-1}|y_1 - x_1| + \sum_{i=2}^d |y_i - x_i| \leq \|\delta\|$ when $h > 1$. By the same logic, in all three cases $\mu(z)$ is maximised at the origin, and so it is straightforward to see that $\sup_{z \in \mathbb{R}^d} \mu(z) < \infty$. \square

Proof of Theorem 2.1. First we show that for all $h \geq h_0$ and all $x, y \in \mathbb{R}^d$ it holds that $q_h^R(x, y) \geq h^{-1}q^R(x, y)$, where $h_0 \geq 1$ is the value defined in Condition 2.1. From (2.5), we have

$$\frac{q_h^R(x, y)}{q^R(x, y)} = h^{-1} \frac{\mu(\delta_h/\sigma)}{\mu(\delta/\sigma)}. \quad (\text{B.1})$$

Condition 2.1 guarantees $\mu(\delta_h/\sigma) \geq \mu(\delta/\sigma)$ for all $h \geq h_0$, which together with (B.1) gives $q_h^R(x, y) \geq h^{-1}q^R(x, y)$. Combining the latter inequality with Lemma A.1 gives

$$\text{Gap}(P_h^R) \geq h^{-1}\text{Gap}(P^R) = \Theta(h^{-1}) \quad \text{as } h \rightarrow \infty.$$

To show that $\text{Gap}(P_h^R) \leq \Theta(h^{-1})$, take $X^{(t)} \sim \pi(\cdot)$ and $X^{(t+1)}|X^{(t)} \sim P_h^R(X^{(t)}, \cdot)$. We consider the set $K := \{y \in \mathbb{R}^d : |y_1| > k\}$, with k chosen such that $0 < \pi(K) < 1/2$ (since $\pi(\cdot)$ is defined on a Polish space, it is tight, meaning this is always possible). Recall from (A.2) that $\text{Gap}(P_h^R) \leq 2\mathbb{P}(X^{(t+1)} \in K^c | X^{(t)} \in K)$. We have

$$\begin{aligned} \mathbb{P}(X^{(t+1)} \in K^c | X^{(t)} \in K) &\leq \mathbb{P}(|X_1^{(t)} + \sigma h \xi_1| \leq k | X^{(t)} \in K) \\ &= \mathbb{P}(-X_1^{(t)} - k \leq \sigma h \xi_1 \leq -X_1^{(t)} + k | X^{(t)} \in K) \\ &\leq (\sigma h)^{-1} 2k \sup_{z \in \mathbb{R}^d} \mu(z), \end{aligned}$$

where ξ_1 is the first component of $\xi \sim \mu$. Condition 2.1 implies $\sup_{z \in \mathbb{R}^d} \mu(z) < \infty$, giving that $\text{Gap}(P_h^R) \leq \Theta(h^{-1})$ for $h \rightarrow \infty$, as desired. \square

Proof of Theorem 2.2. This follows directly from the proof of Theorem 2.4 below, by noting that setting $L = 1$ in Hamiltonian Monte Carlo gives the Langevin algorithm. \square

Proof of Theorem 2.3. Take $\sigma = 1$ for simplicity of notation (or otherwise replace h by σh). Let $(X^{(t)})_{t=1}^\infty$ be the MALA chain started in stationarity. We consider the sets $A_h := \{y \in \mathbb{R}^d : |y_1| \leq h^{1/(2\tilde{\gamma})}\}$, where $\tilde{\gamma} = \max\{1, \gamma\}$, and $K := \{y \in \mathbb{R}^d : |y_1| > k\}$, with k chosen such that $0 < \pi(K) < 1/2$. Also, given

$$\epsilon \in \left(0, \liminf_{|x_1| \rightarrow \infty} \left(\inf_{(x_2, \dots, x_d) \in \mathbb{R}^{d-1}} \left| \frac{\partial \log \pi(x)}{\partial x_1} \right| \|x\|^\gamma \right) \right),$$

Condition 2.3(ii) implies that we can choose k large enough such that

$$\inf_{(x_2, \dots, x_d) \in \mathbb{R}^{d-1}} \left| \frac{\partial \log \pi(x)}{\partial x_1} \right| \|x\|^\gamma \geq \epsilon \quad \text{for all } x \in K.$$

We will now show $\Pr(X^{(t+1)} \in K^c | X^{(t)} \in K) \leq \Theta(e^{-h^\alpha})$ for some $\alpha > 0$. Note that

$$\begin{aligned} \mathbb{P}(X^{(t+1)} \in K^c | X^{(t)} \in K) &= \mathbb{P}(X^{(t+1)} \in K^c | X^{(t)} \in K \cap A_h) \mathbb{P}(X^{(t)} \in K \cap A_h) \\ &\quad + \mathbb{P}(X^{(t+1)} \in K^c | X^{(t)} \in K \cap A_h^c) \mathbb{P}(X^{(t)} \in K \cap A_h^c), \end{aligned}$$

meaning that

$$\mathbb{P}(X^{(t+1)} \in K^c | X^{(t)} \in K) \leq \mathbb{P}(X^{(t+1)} \in K^c | X^{(t)} \in K \cap A_h) + \mathbb{P}(X^{(t)} \in K \cap A_h^c).$$

Condition 2.3(ii) implies $\mathbb{P}(X^{(t)} \in K \cap A_h^c) \leq \mathbb{P}(X^{(t)} \in A_h^c) \leq \Theta(e^{-h^{\beta/(2\tilde{\gamma})}})$.

Also, given $Y = (Y_1, \dots, Y_d)$ with $Y|X^{(t)} \sim Q_h^M(X^{(t)}, \cdot)$, we have

$$Pr(X^{(t+1)} \in K^c | X^{(t)} \in K \cap A_h) \leq Pr(|Y_1| \leq k | X^{(t)} \in K \cap A_h).$$

Denote $\frac{\partial}{\partial x_1} \log \pi(x)$ by $\partial_1(x)$ for brevity. If $X^{(t)} \in K \cap A_h$ we have $|X_1^{(t)}| \leq h^{1/(2\tilde{\gamma})} \leq h^{1/2}$ and

$$|\partial_1(X^{(t)})| \geq \epsilon \|X^{(t)}\|^{-\gamma} \geq \epsilon h^{-\gamma/(2\tilde{\gamma})} \geq \epsilon h^{-1/2},$$

which imply

$$\begin{aligned} |Y_1| &= |X_1^{(t)} + h^2 \partial_1(X^{(t)}) + h \xi_1| \\ &\geq h^2 |\partial_1(X^{(t)})| - h |\xi_1| - |X_1^{(t)}| \\ &\geq h^{3/2} \epsilon - h |\xi_1| - h^{1/2}, \end{aligned}$$

where $\xi_1 \sim N(0, 1)$. It follows that

$$\begin{aligned} Pr(|Y_1| \leq k | X^{(t)} \in K \cap A_h) &\leq Pr(h^{3/2} \epsilon - h |\xi_1| - h^{1/2} \leq k | X^{(t)} \in K \cap A_h) \\ &= Pr(|\xi_1| \geq \epsilon h^{1/2} - h^{-1/2} - k h^{-1}). \end{aligned}$$

Since $Pr(|\xi_1| \geq t) \leq \exp(-t^2/2)$ for every $t > 0$ and $\epsilon h^{1/2} - h^{-1/2} - k h^{-1} \geq 2h^{1/3}$ eventually as $h \rightarrow \infty$, it follows

$$Pr(|Y_1| \leq k | X^{(t)} \in K \cap A_h) \leq \Theta(e^{-h^{2/3}}) \quad \text{as } h \rightarrow \infty.$$

Combining the inequalities above it follows that $\mathbb{P}(X^{(t+1)} \in K^c | X^{(t)} \in K) \leq \Theta(e^{-h^\alpha})$ for $\alpha = \max\{\beta/(2\tilde{\gamma}), 2/3\} > 0$ as $h \rightarrow \infty$. Finally, using the conductance bound in (A.2) we have $\text{Gap}(P_h^M) \leq \Theta(e^{-h^\alpha})$ as $h \rightarrow \infty$. \square

Proof of Theorem 2.4. Fix $\delta \in (0, (1-q)/2)$ with q defined in Condition 2.2 and consider the sets $A_h := \{y \in \mathbb{R}^d : |y_1| < k + h\}$ and $K := \{y \in \mathbb{R}^d : |y_1| > k\}$. Here k is chosen large enough that Lemma B.1 below is satisfied and that $0 < \pi(K) < 1/2$, which can always be done thanks to the tightness and positiveness of π (see above). Lemma B.1 implies that if $X^{(t)} \in K \cap A_h$, $|\xi_1| \leq h^{1-\delta}$ and $h \geq h_0$, with h_0 defined in the proposition, then $X^{(t+1)} \in K$. We will now upper bound the probability $\mathbb{P}(X^{(t+1)} \in K^c | X^{(t)} \in K)$. First note that

$$\begin{aligned} \mathbb{P}(X^{(t+1)} \in K^c | X^{(t)} \in K) &= \mathbb{P}(X^{(t+1)} \in K^c | X^{(t)} \in K \cap A_h) \mathbb{P}(X^{(t)} \in K \cap A_h) \\ &\quad + \mathbb{P}(X^{(t+1)} \in K^c | X^{(t)} \in K \cap A_h^c) \mathbb{P}(X^{(t)} \in K \cap A_h^c), \end{aligned}$$

which implies

$$\begin{aligned} \mathbb{P}(X^{(t+1)} \in K^c | X^{(t)} \in K) &\leq \mathbb{P}(X^{(t+1)} \in K^c | X^{(t)} \in K \cap A_h) \\ &\quad + \mathbb{P}(X^{(t)} \in K \cap A_h^c). \end{aligned}$$

Breaking out the first term on the right-hand side gives

$$\begin{aligned} \mathbb{P}(X^{(t+1)} \in K^c | X^{(t)} \in K \cap A_h) &\leq \\ \mathbb{P}(X^{(t+1)} \in K^c | X^{(t)} \in K \cap A_h, |\xi_1| \leq h^{1-\delta}) &+ \mathbb{P}(|\xi_1| > h^{1-\delta}), \end{aligned}$$

which, using the result of Lemma B.1, reduces to

$$\mathbb{P}(X^{(t+1)} \in K^c | X^{(t)} \in K \cap A_h) \leq \mathbb{P}(|\xi_1| > h^{1-\delta}).$$

Hence we obtain the overall bound

$$\mathbb{P}(X^{(t+1)} \in K^c | X^{(t)} \in K) \leq \mathbb{P}(|\xi_1| > h^{1-\delta}) + \mathbb{P}(X^{(t)} \in K \cap A_h^c).$$

Using standard bounds on Gaussian tails and $\xi_1 \sim N(0, 1)$, we have $\mathbb{P}(|\xi_1| > h^{1-\delta}) \leq \exp(-h^{2(1-\delta)}/2)$. Also, from Lemma B.3, we have $\mathbb{P}(X^{(t)} \in K \cap A_h^c) \leq \Theta(e^{-\gamma h^{1+q}-q \log(h)})$ as $h \rightarrow \infty$ for some $\gamma \in (0, \infty)$. Hence, since $\delta < (1 - q)/2$, we obtain

$$\mathbb{P}(X^{(t+1)} \in K^c | X^{(t)} \in K) \leq \Theta\left(e^{-\gamma h^{1+q}-q \log(h)}\right) \quad \text{as } h \rightarrow \infty.$$

Finally, the conductance bound in (A.2) gives

$$\text{Gap}(P_h^H) \leq \Theta\left(e^{-\gamma h^{1+q}-q \log(h)}\right) \quad \text{as } h \rightarrow \infty.$$

□

Proof of Proposition 2.2. Write f_1 and f_2 for the densities of two Gaussian measures $G_1(\cdot)$ and $G_2(\cdot)$ on \mathbb{R} , with means μ_1 and μ_2 respectively, and common variance c^2 . Without loss of generality set $\mu_2 \geq \mu_1$. It is well-known that the Total Variation distance between these can be written $\int_{f_1 \geq f_2} (f_1(x) - f_2(x)) dx$, and straightforward to see that $f_1(x) \geq f_2(x)$ if and only if $x \leq \mu_1 + (\mu_1 + \mu_2)/2$. Simple calculations then reveal that

$$\|G_1(\cdot) - G_2(\cdot)\|_{TV} = 2\Phi^*(\tau/2) - 1,$$

where Φ^* denotes the standard Gaussian cumulative distribution function, and

$$\tau := |c^{-1}(\mu_2 - \mu_1)|.$$

Inserting $c = h$, $\mu_1 = x$ and $\mu_2 = x + (h^2/2)\nabla \log \pi(x)$ then gives the result. □

B.1.1 Lemmas used to prove Theorem 2.4

Lemma B.1. *Assume Condition 2.2 and let $\delta \in (0, 1)$. For every $L \geq 1$ there exist large enough k and h_0 such that for every $h \geq h_0$, $|\xi_1| \leq h^{1-\delta}$ and $|x_1(0)| \in [k, k + h)$ it holds that $|x_1(L)| \geq k$, where $x(L)$ is defined in (2.10).*

Proof. Recall that, for each $i \geq 1$, $x_1(i)$ is implicitly a function of the starting location $x_1(0)$, the step-size h and the noise ξ_1 . In order to prove the thesis it is sufficient to show that for fixed, sufficiently large $k > 0$ we have

$$\inf_{\xi_1, x_1(0)} |x_1(L)| \rightarrow \infty \quad \text{as } h \uparrow \infty, \quad (\text{B.2})$$

where ξ_1 and $x_1(0)$ in the infimum are restricted as in the lemma's statement, i.e. $\xi_1 \in (-h^{1-\delta}, h^{1-\delta})$ and $x_1(0) \in (-(k + h), -k] \cup [k, k + h)$. In order to prove (B.2) we will show that for all $i \geq 1$, as $h \uparrow \infty$ we have

$$\Theta(h^{2 \sum_{j=0}^{i-1} q^j}) \leq \inf |x_1(i)| \leq \sup |x_1(i)| \leq \Theta(h^{q^{i+2} \sum_{j=0}^{i-1} q^j}), \quad (\text{B.3})$$

$$\Theta(h^{2 \sum_{j=1}^i q^j}) \leq \inf |\partial_1(i)| \leq \sup |\partial_1(i)| \leq \Theta(h^{q^{i+1} + 2 \sum_{j=1}^i q^j}), \quad (\text{B.4})$$

where infima and suprema run over $\xi_1 \in (-h^{1-\delta}, h^{1-\delta})$ and $x_1(0) \in (-(k + h), -k] \cup [k, k + h)$ as in (B.2), and $\partial_1(i)$ stands for $\partial \log \pi_1 / \partial x_1(x_1(i))$. Note that, for any $i \geq 1$, (B.4) is implied by (B.3) thanks to $\inf |x_1(1)| \rightarrow \infty$ as $h \rightarrow \infty$ and (2.7). Thus it suffices to prove that (B.3) holds for all $i \geq 1$, which we will do by induction over i .

In the following, k is chosen large enough that $c|x_1|^q \leq |\partial \log \pi_1 / \partial x_1(x_1)| \leq C|x_1|^q$ for some $0 < c \leq C < \infty$ and all $|x_1| > k$, which can be done by (2.7). Also, unless otherwise stated, we assume $\xi_1 \in (-h^{1-\delta}, h^{1-\delta})$ and $x_1(0) \in (-(k+h), -k] \cup [k, k+h)$, and all infima and suprema are taken over those sets.

Considering $i = 1$, we have $x_1(1) = x_1(0) + h\xi_1 + (h^2/2)\partial_1(0)$, which implies

$$\frac{h^2}{2}|\partial_1(0)| - |x_1(0)| - h|\xi_1| \leq |x_1(1)| \leq \frac{h^2}{2}|\partial_1(0)| + |x_1(0)| + h|\xi_1|.$$

Then, since $|\xi_1| \in (0, h^{1-q})$, $|x_1(0)| \in [k, k+h)$ and $ck^q \leq c|x_1(0)|^q \leq |\partial_1(0)| \leq C|x_1(0)|^q \leq C(h+k)^q$, we have

$$\Theta(h^2) = \frac{h^2}{2}ck^q - (k+h) \leq |x_1(1)| \leq \frac{h^2}{2}C(h+k)^q + (k+h) + h^{2-q} = \Theta(h^{2+q})$$

meaning that (B.3) is satisfied for $i = 1$.

We then show that if (B.3) and (B.4) hold for $i = 1, \dots, \ell - 1$, where $\ell \geq 2$, then they also hold for $i = \ell$. First note that when $\ell \geq 2$, (2.10) implies

$$x_1(\ell) = x_1(\ell - 1) + h\xi_1 + \frac{h^2}{2}\partial_1(0) + h^2 \sum_{j=1}^{\ell-1} \partial_1(j). \quad (\text{B.5})$$

From (B.5) and $|\xi_1| \in (0, h^{1-q})$, we can deduce that

$$h^2|\partial_1(\ell - 1)| - |x_1(\ell - 1)| - h^2 \sum_{j=0}^{\ell-2} |\partial_1(j)| \leq |x_1(\ell)| \leq |x_1(\ell - 1)| + h^{2-q} + h^2 \sum_{j=0}^{\ell-1} |\partial_1(j)|. \quad (\text{B.6})$$

Combining the lower bound in (B.6) with (B.3) and (B.4) for $i = 1, \dots, \ell - 1$ we obtain

$$\begin{aligned} \inf |x_1(\ell)| &\geq \inf h^2|\partial_1(\ell - 1)| - \sup \left(|x_1(\ell - 1)| + h^2 \sum_{j=0}^{\ell-2} |\partial_1(j)| \right) \\ &\geq \Theta(h^{2 \sum_{j=0}^{\ell-1} q^j}) - \Theta(h^{q^{\ell-1} + 2 \sum_{j=0}^{\ell-2} q^j}) = \Theta(h^{2 \sum_{j=0}^{\ell-1} q^j}), \end{aligned}$$

where the last equality follows from $q^{\ell-1} + 2 \sum_{j=0}^{\ell-2} q^j \leq 2 \sum_{j=0}^{\ell-1} q^j$. Thus the lower bound in (B.3) holds also for $i = \ell$. Similarly, combining the upper bound in (B.6) with (B.3) and (B.4) for $i = 1, \dots, \ell - 1$ we obtain

$$\begin{aligned} \sup |x_1(\ell)| &\leq \sup \left(|x_1(\ell - 1)| + h^{2-q} + h^2 \sum_{j=0}^{\ell-1} |\partial_1(j)| \right) \\ &\leq \Theta(h^{q^{\ell-1} + 2 \sum_{j=0}^{\ell-2} q^j} + h^{2-q} + h^{q^i + 2 \sum_{j=0}^{\ell-1} q^j}) = \Theta(h^{q^i + 2 \sum_{j=0}^{\ell-1} q^j}), \end{aligned}$$

where the last equality follows from $2 - q \leq q^{\ell-1} + 2 \sum_{j=0}^{\ell-2} q^j \leq q^i + 2 \sum_{j=0}^{\ell-1} q^j$. Thus the upper bound in (B.3) holds also for $i = \ell$ and the proof is complete. \square

Lemma B.2. *Condition 2.2 (ii) implies that there exist t, c and C in $(0, \infty)$ such that*

$$\pi_1(x_1) \leq Ce^{-c|x_1|^{1+q}}, \quad \text{for all } |x_1| \geq t. \quad (\text{B.7})$$

Proof. Condition 2.2 implies that there exists $t, c \in (0, \infty)$ such that

$$\left| \frac{d}{dx_1} \log \pi_1(x_1) \right| \geq c|x_1|^{1+q}, \quad \text{for all } |x_1| \geq t.$$

Since $\log \pi_1 \in C_1(\mathbb{R})$, the above implies that either

$$\frac{d}{dx_1} \log \pi_1(x_1) > cx_1^{1+q} \quad \text{or} \quad \frac{d}{dx_1} \log \pi_1(x_1) < -cx_1^{1+q},$$

holds for all $|x_1| \geq t$. Since $\int \pi_1(x_1) dx_1 = 1$ the latter option must be true. Computing the anti-derivative gives

$$\log \pi_1(x_1) \leq -cx_1^{1+q} + \log C,$$

for some constant $\log C$. An analogous argument can be used in the case $x_1 \downarrow -\infty$, and the two combined give the result. \square

Lemma B.3. *If Condition 2.2 holds and $X_1 \sim \pi_1(\cdot)$, then there exists $\gamma \in (0, \infty)$ such that*

$$\mathbb{P}(|X_1| > k + h) \leq \Theta \left(e^{-\gamma h^{1+q} - q \log(h)} \right) \quad \text{as } h \rightarrow \infty.$$

Proof. Using Lemma B.2, provided $k + h > t$ we have

$$\begin{aligned} \mathbb{P}(|X_1| > k + h) &= \int_{k+h}^{\infty} \pi_1(x_1) dx_1 + \int_{-\infty}^{-(k+h)} \pi_1(x_1) dx_1 \\ &\leq 2C \int_{k+h}^{\infty} e^{-cx_1^{1+q}} dx_1 \\ &= 2C \frac{c^{-1/(q+1)}}{q+1} \Gamma \left(\frac{1}{1+q}, c(k+h)^{1+q} \right), \end{aligned}$$

where $\Gamma(a, b) := \int_b^{\infty} u^{a-1} e^{-u} du$ is the incomplete Gamma function. For the case $q > 0$ the upper bound of Gautschi [1959], which is described on pages 771-772 of Alzer [1997], states that for fixed $a \in (0, 1)$ and $x > 0$ we have

$$\Gamma(a, x^{-a}) \leq e^{-x^{-a}} \frac{c_a}{a} \left((x^{-a} + c_a^{-1})^a - x \right),$$

where $c_a := \Gamma(1+a)^{1/(1-a)}$. Setting $C_2 := 2C c^{-1/(q+1)}/(q+1)$, $a := 1/(1+q)$ and using this upper bound gives

$$\mathbb{P}(|X_1| > k + h) \leq e^{-c(k+h)^{1+q}} C_2 \frac{c_a}{a} \left[\left(c(k+h)^{\frac{1}{a}} + c_a^{-1} \right)^a - c^a(k+h) \right].$$

We use a Taylor series expansion of $f(c(k+h)^{1/a} + c_a^{-1})$ about $f(c(k+h)^{1/a})$, where $f(x) = x^a$. The terms each have a different power of h . This gives

$$(c(k+h)^{\frac{1}{a}} + c_a^{-1})^a = c^a(k+h) + c_a^{-1} a (c(k+h)^{\frac{1}{a}})^{a-1} + O(h^{(a-2)/a})$$

Since $a = 1/(1+q) < 1$ then $(a-1)/a = -q$ and $(a-2)/a = -(1+2q)$, and therefore

$$(c(k+h)^{\frac{1}{a}} + c_a^{-1})^a - c^a(k+h) = \Theta((c(k+h)^{\frac{1}{a}})^{a-1}) = \Theta(h^{-q}).$$

Combining with the above, we can write that for any fixed k and fixed $q > 0$, there exists $\gamma \in (0, \infty)$ such that as $h \uparrow \infty$

$$\mathbb{P}(|X_1| > k + h) \leq \Theta \left(e^{-\gamma h^{1+q} - q \log(h)} \right).$$

In the case $q = 0$ the integral $\int_{k+h}^{\infty} e^{-cx_1} dx_1 = e^{-c(k+h)}/c$ and the result is immediate. \square

B.2 Proofs for Section 3

Proof of Proposition 3.1. Since $\nabla \log \pi(x) = a$ for every $x \in \mathbb{R}^d$, it follows that the normalizing constant, Z , of $q(x, y)$ in (3.2) is independent of x . First we show that $g(t) = tg(1/t)$ implies reversibility. From the symmetry of μ_σ and $g(t) = tg(1/t)$ it follows

$$\begin{aligned}\pi(x)q(x, y) &= \exp(a^T x + b)Z^{-1}g\left(\exp\left(a^T(y - x)\right)\right)\mu_\sigma(x, y) \\ &= \exp(a^T x + b)Z^{-1}\exp\left(a^T(y - x)\right)g\left(\exp\left(-a^T(y - x)\right)\right)\mu_\sigma(y, x) \\ &= \pi(y)q(y, x),\end{aligned}$$

which implies that q is π -reversible. Conversely, if q is π -reversible, then

$$1 = \frac{\pi(x)q(x, y)}{\pi(y)q(y, x)} = \frac{\exp(a^T(x - y))g\left(1/\exp\left(a^T(x - y)\right)\right)}{g\left(\exp\left(a^T(x - y)\right)\right)} = \frac{tg(1/t)}{g(t)},$$

for $t = \exp(a^T(x - y))$. For $a \neq 0$, $\exp(a^T(x - y))$ takes any positive value as $x, y \in \mathbb{R}^d$ and thus we have $g(t) = tg(1/t)$ for every $t > 0$. \square

Proof of Proposition 3.2. Define the set $A := \{x \in \mathbb{R}^d : x_1 \geq 0\}$, and note that $A \cup A^c = \mathbb{R}^d$ and $\int_A \mu_\sigma(z)dz = 1/2$. Setting $y - x = z$, then $t(z) = e^{z^T \nabla \log \pi(x)}$ and $1/t(z) = e^{-z^T \nabla \log \pi(x)} = t(-z)$, meaning

$$\begin{aligned}Z(x) &= \int_{\mathbb{R}^d} \frac{t(z)}{1 + t(z)} \mu_\sigma(z) dz \\ &= \int_A \left(\frac{t(z)}{1 + t(z)} \mu_\sigma(z) + \frac{t(-z)}{1 + t(-z)} \mu_\sigma(-z) \right) dz.\end{aligned}$$

Noting that $\mu_\sigma(z) = \mu_\sigma(-z)$ and $t(-z) = 1/t(z)$ then gives

$$Z(x) = \int_A \mu_\sigma(z) dz = \frac{1}{2}$$

which completes the proof. \square

Proof of Proposition 3.3. Assume $y = x + b(x, z) \times z$ is generated using Algorithm 1. Then for any $A \in \mathcal{B}(\mathbb{R})$

$$\mathbb{P}[y \in A] = \mathbb{P}[\{z \in A\} \cap \{b(x, z) = 1\}] + \mathbb{P}[\{-z \in A\} \cap \{b(x, z) = -1\}].$$

Note that the second term on the right-hand side can be re-written

$$\mathbb{P}[\{z \in A\} \cap \{b(x, -z) = -1\}],$$

owing to the symmetry of μ_σ . Because of this, we can write

$$\begin{aligned}\mathbb{P}[y \in A] &= \int_A \frac{e^{z^T \nabla \log \pi(x)}}{1 + e^{z^T \nabla \log \pi(x)}} \mu_\sigma(z) dz + \int_A \frac{1}{1 + e^{-z^T \nabla \log \pi(x)}} \mu_\sigma(z) dz \\ &= 2 \int_A \frac{e^{z^T \nabla \log \pi(x)}}{1 + e^{z^T \nabla \log \pi(x)}} \mu_\sigma(z) dz \\ &= Q^B(x, A)\end{aligned}$$

which completes the proof. \square

Proof of Proposition 3.4. We establish a point-wise bound on the candidate transition densities of the two algorithms. Combining this with Lemma A.1 gives an equivalent bound on the spectral gaps. To reach this point-wise bound, first note that the candidate transition density associated with the Random Walk algorithm is $q^R(x, x+z) = \mu_\sigma(z)$ for any $x, z \in \mathbb{R}^d$. Now, for the modified Barker proposal, the candidate density can be written

$$\begin{aligned}\tilde{q}^B(x, x+z) &= \mu_\sigma(z)\tilde{p}(x, z) + \mu_\sigma(-z)(1 - \tilde{p}(x, -z)) \\ &= \mu_\sigma(z)(\tilde{p}(x, z) - \tilde{p}(x, -z) + 1) \\ &= 2\tilde{p}(x, z)\mu_\sigma(z),\end{aligned}$$

where on the last line we have used that $\tilde{p}(x, -z) = 1 - \tilde{p}(x, z)$. Noting that $\tilde{p}(x, z) \leq 1$ establishes that $q^R(x, x+z) \geq \tilde{q}^B(x, x+z)/2$ for any $x, z \in \mathbb{R}^d$, and upon combining this with Lemma A.1 the result follows. \square

B.3 Proofs for Section 4

Interestingly, the proof of the lower bound of Theorem 4.1 is analogous to the one of Theorem 2.1, providing further insight into the similarity between the Barker scheme and random walk in terms of robustness to scales.

Proof of Theorem 4.1. Let q_h^B be the proposal pdf defined in (4.1), with $q^B = q_1^B$ being the pdf of Q^B . It follows from (4.1) that

$$\frac{q_h^B(x, y)}{q^B(x, y)} = h^{-1} \frac{\mu(\delta_h/\sigma)}{\mu(\delta/\sigma)}, \quad (\text{B.8})$$

where δ and δ_h are defined in (2.4) and above. Note that the expression above coincides with the expression for the random walk proposals in (B.1), i.e. $\frac{q_h^B(x, y)}{q^B(x, y)} = \frac{q_h^R(x, y)}{q^R(x, y)}$. Thus, arguing as in the proof of Theorem 2.1, we have that for all $h \geq h_0$ and all $x, y \in \mathbb{R}^d$ it holds that $q_h^B(x, y) \geq h^{-1}q^B(x, y)$, where $h_0 \geq 1$ is the value defined in Condition 2.1. Combining the latter inequality with Lemma A.1 gives

$$\text{Gap}(P_h^B) \geq h^{-1}\text{Gap}(P^B) = \Theta(h^{-1}) \quad \text{as } h \rightarrow \infty.$$

To show that $\text{Gap}(P_h^B) \leq \Theta(h^{-1})$, note that $q_h^B(x, y) \leq 2^d q_h^R(x, y)$ for all $x, y \in \mathbb{R}^d$ by (4.1) and (2.3). Thus, Lemma A.1 and Theorem 2.1 give $\text{Gap}(P_h^B) \leq 2^d \text{Gap}(P_h^R) = \Theta(h^{-1})$ as $h \uparrow \infty$. \square

B.3.1 Proof of Theorem 4.2

The following lemma, which is an extension of Theorem 4.1 of [Roberts and Tweedie, 1996], provides generic sufficient conditions for the geometric ergodicity of Metropolis–Hastings algorithms.

Lemma B.4. *Let P be a ϕ -irreducible and aperiodic Metropolis–Hastings kernel on \mathbb{R}^d with proposal Q such that compact sets are small under P . If there exist a function $V : \mathbb{R}^d \rightarrow (0, \infty)$ such that $\sup_{x \in \mathbb{R}^d} \frac{QV(x)}{V(x)} < \infty$ and*

$$\liminf_{\|x\| \rightarrow +\infty} \int_{\mathbb{R}^d} q(x, y) \alpha(x, y) dy > \limsup_{\|x\| \rightarrow \infty} \frac{QV(x)}{V(x)}, \quad (\text{B.9})$$

then P is π -a.e. geometrically ergodic.

Proof. We show that (B.9) implies the following Foster-Lyapunov drift conditions:

$$\sup_{x \in \mathbb{R}^d} \frac{PV(x)}{V(x)} < \infty \text{ and } \limsup_{\|x\| \rightarrow \infty} \frac{PV(x)}{V(x)} < 1,$$

which imply π -a.e. geometric ergodicity (see e.g. Theorem 3.1 and Lemma 3.5 of Jarner and Hansen [2000]). First note that

$$\begin{aligned} \frac{PV(x)}{V(x)} &= \int_{\mathbb{R}^d} \left(\frac{V(y)}{V(x)} \alpha(x, y) + 1 - \alpha(x, y) \right) q(x, y) dy \\ &\leq \int_{\mathbb{R}^d} \frac{V(y)}{V(x)} q(x, y) dy + \int_{\mathbb{R}^d} (1 - \alpha(x, y)) q(x, y) dy \leq \frac{QV(x)}{V(x)} + 1, \end{aligned}$$

which implies $\sup_{x \in \mathbb{R}^d} \frac{PV(x)}{V(x)} \leq \sup_{x \in \mathbb{R}^d} \frac{QV(x)}{V(x)} + 1 < \infty$. Also, the inequalities above imply

$$\frac{PV(x)}{V(x)} \leq 1 - \left(\int_{\mathbb{R}^d} \alpha(x, y) q(x, y) dy - \frac{QV(x)}{V(x)} \right). \quad (\text{B.10})$$

From (B.9) we have

$$\begin{aligned} 0 &< \liminf_{\|x\| \rightarrow +\infty} \int_{\mathbb{R}^d} q(x, y) \alpha(x, y) dy - \limsup_{\|x\| \rightarrow \infty} \frac{QV(x)}{V(x)} \\ &\leq \liminf_{\|x\| \rightarrow +\infty} \left(\int_{\mathbb{R}^d} q(x, y) \alpha(x, y) dy - \frac{QV(x)}{V(x)} \right). \end{aligned} \quad (\text{B.11})$$

Combining (B.10) and (B.11) we obtain $\limsup_{\|x\| \rightarrow \infty} \frac{PV(x)}{V(x)} < 1$, as desired. \square

We will show that the conditions of Lemma B.4 are satisfied when considering a Lyapunov function $V_s(x) = \exp(s\|x\|_\infty)$ based on the sup norm, $\|x\|_\infty = \sup_i |x_i|$.

In the following results we denote $\sup_{t>0} g(t)$ by M . We denote the log-target and its derivatives as $U(x) = \log \pi(x)$ and $U_i(x) = \frac{\partial}{\partial x_i} U(x)$, respectively. Condition 4.1 implies that $\nabla U(x) = f'(\|x\|) \frac{x}{\|x\|}$ and $U_i(x) = f'(\|x\|) \frac{x_i}{\|x\|}$ for $\|x\| > R$. Also, we denote the kernel $Q^{(g)}$ in (4.2) as Q for brevity and its density function as

$$q(x, y) = \prod_{i=1}^d \frac{g(e^{w_i U_i(x)}) \mu_\sigma(w)}{Z_i(x)} = \prod_{i=1}^d q_i(w_i; x), \quad (\text{B.12})$$

where $w_i = y_i - x_i$ and $q_i(w_i; x) = g(e^{w_i U_i(x)}) \mu_\sigma(w) / Z_i(x)$.

First, we provide some simple results on the behaviour of g , Z_i and q_i that will be useful afterwards.

Lemma B.5. *Let $g : (0, \infty) \rightarrow (0, \infty)$ be bounded, non-decreasing and such that $g(t) = tg(1/t)$ for all $t > 0$. Then $g(t) \geq g(1) \min\{1, t\}$ and $\frac{g(1)}{2} \leq Z_i(x) \leq M$, where $M = \sup_{t>0} g(t)$.*

Proof. If $t \geq 1$ then $g(t) \geq g(1) = g(1) \min\{1, t\}$ by the monotonicity of g . If $t < 1$ then $g(t) = tg(1/t) \geq tg(1) = g(1) \min\{1, t\}$ by $g(t) = tg(1/t)$ and the monotonicity of g . From $Z_i(x) = \int_{\mathbb{R}} g(e^{w_i U_i(x)}) \mu_\sigma(w) dw$ and $g(t) \leq M$ it follows $Z_i(x) \leq M$. If $U_i(x) \leq 0$, then $g(e^{w_i U_i(x)}) \geq g(1)$ for all $w \leq 0$ and thus $Z_i(x) \geq \int_{-\infty}^0 g(1) \mu_\sigma(w) dw = \frac{g(1)}{2}$. The case $U_i(x) \geq 0$ is analogous. \square

Lemma B.6. *If g is bounded and non-decreasing, then $Z_i(x) \rightarrow \frac{M}{2}$ as $U_i(x) \rightarrow -\infty$ or $U_i(x) \rightarrow +\infty$ and for all $w_i \in \mathbb{R}$ it holds*

$$\begin{aligned} q_i(w_i; x) &\rightarrow 2\mu_\sigma(w_i) \mathbb{I}_{(-\infty, 0]}(w_i) & \text{as } U_i(x) \rightarrow -\infty \text{ and} \\ q_i(w_i; x) &\rightarrow 2\mu_\sigma(w_i) \mathbb{I}_{[0, +\infty)}(w_i) & \text{as } U_i(x) \rightarrow +\infty. \end{aligned}$$

Proof. Consider the case $U_i(x) \rightarrow -\infty$. From $g(t) = t g(1/t) \leq tM$ it follows $g(t) \rightarrow 0$ as $t \rightarrow 0$. Also, from the boundedness and monotonicity of g it holds $g(t) \rightarrow M$ as $t \rightarrow \infty$. Therefore, for all $w_i \in \mathbb{R}$,

$$g(\exp(w_i U_i(x))) \rightarrow M \mathbb{I}_{(-\infty, 0]}(w_i) \quad \text{as } U_i(x) \rightarrow -\infty. \quad (\text{B.13})$$

Thus, from the bounded convergence theorem $Z_i(x) \rightarrow \int_{-\infty}^0 M \mu_\sigma(w_i) dw_i = \frac{M}{2}$ as $U_i(x) \rightarrow -\infty$ and, consequently, $q_i(w_i; x) \rightarrow 2\mu_\sigma(w_i) \mathbb{I}_{(-\infty, 0]}(w_i)$ as $U_i(x) \rightarrow -\infty$. The case $U_i(x) \rightarrow +\infty$ is analogous. \square

We now provide two lemmas that will be used to prove the inequality in (B.9).

Lemma B.7. *Suppose Condition 4.1 holds. Let $V_s(x) = \exp(s\|x\|_\infty)$ and Q the kernel with density q as in (B.12). Then*

$$\inf_{s>0} \limsup_{\|x\| \rightarrow \infty} \frac{Q V_s(x)}{V_s(x)} = 0.$$

Proof. Let $x \in \mathbb{R}^d$ and $Y \sim Q(x, \cdot)$. Since $V_s(y) \leq \sum_{i=1}^d \exp(s|y_i|)$ we have

$$\mathbb{E} \left[\frac{V_s(Y)}{V_s(x)} \right] \leq \sum_{i=1}^d \mathbb{E} \left[\frac{e^{s|Y_i|}}{e^{s\|x\|_\infty}} \right].$$

We now bound $\mathbb{E} [e^{s(|Y_i| - \|x\|_\infty)}]$ differently depending on whether $|x_i| \leq \frac{1}{2}\|x\|_\infty$ or $\frac{1}{2}\|x\|_\infty < |x_i| \leq \|x\|_\infty$.

If $|x_i| \leq \frac{1}{2}\|x\|_\infty$ it follows from the triangle inequality that $|x_i + w| - \|x\|_\infty \leq |x_i| + |w| - \|x\|_\infty \leq |w| - \|x\|_\infty/2$ for any $w \in \mathbb{R}$. Also, from (B.12) and Lemma B.5 we have $q_i(w_i; x) \leq \frac{2M}{g(1)} \mu_\sigma(w_i)$. It follows

$$\mathbb{E} [e^{s(|Y_i| - \|x\|_\infty)}] \mathbb{I} \left(|x_i| \leq \frac{\|x\|_\infty}{2} \right) \leq \frac{2M}{g(1)} e^{-s\|x\|_\infty/2} \int_{\mathbb{R}} e^{s|w|} \mu_\sigma(w) dw,$$

and thus

$$\limsup_{\|x\| \rightarrow \infty} \mathbb{E} [e^{s(|Y_i| - \|x\|_\infty)}] \mathbb{I} \left(|x_i| \leq \frac{\|x\|_\infty}{2} \right) = 0. \quad (\text{B.14})$$

If $\frac{1}{2}\|x\|_\infty < |x_i| \leq \|x\|_\infty$ we have

$$\begin{aligned} \mathbb{E} [e^{s(|Y_i| - \|x\|_\infty)}] \mathbb{I} \left(|x_i| > \frac{\|x\|_\infty}{2} \right) &\leq \\ &\mathbb{I} \left(|x_i| > \frac{\|x\|_\infty}{2} \right) \int_{\mathbb{R}} e^{s(|x_i + w| - |x_i|)} q_i(w; x) dw. \end{aligned}$$

If $\|x\| \rightarrow \infty$ and $|x_i| > \frac{\|x\|_\infty}{2}$ it follows $|x_i| \rightarrow \infty$. Moreover, by Condition 4.1 and $|x_i| > \frac{\|x\|_\infty}{2}$, we have $U_i(x) \leq \frac{f(\|x\|)}{2} \rightarrow -\infty$ as $x_i \rightarrow +\infty$ and $U_i(x) \geq -\frac{f(\|x\|)}{2} \rightarrow +\infty$ as $x_i \rightarrow -\infty$. Therefore, by Lemma B.6

$$\limsup_{\|x\| \rightarrow \infty} \mathbb{I} \left(|x_i| > \frac{\|x\|_\infty}{2} \right) \int_{\mathbb{R}} e^{s(|x_i + w| - |x_i|)} q_i(w; x) dw \leq 2 \int_{-\infty}^0 e^{sw} \mu_\sigma(w) dw.$$

Combining the last two displayed equations we get

$$\limsup_{\|x\| \rightarrow \infty} \mathbb{E} [e^{s(|Y_i| - \|x\|_\infty)}] \mathbb{I} \left(|x_i| > \frac{\|x\|_\infty}{2} \right) \leq 2 \int_{-\infty}^0 e^{sw} \mu_\sigma(w) dw. \quad (\text{B.15})$$

From (B.14), (B.15) and basic properties of the lim sup we get

$$\limsup_{\|x\| \rightarrow \infty} \mathbb{E} \left[e^{s(|Y_i| - \|x\|_\infty)} \right] \leq 2 \int_{-\infty}^0 e^{sw} \mu_\sigma(w) dw.$$

Thus

$$\limsup_{\|x\| \rightarrow \infty} \mathbb{E} \left[\frac{V_s(Y)}{V_s(x)} \right] \leq d \left(\int_{-\infty}^0 e^{sw} 2\mu_\sigma(w) dw \right)$$

which goes to 0 as $s \rightarrow \infty$. \square

Lemma B.8. Assume that $\inf_{w \in (-\delta, \delta)} \mu_\sigma(w) > 0$ for some $\delta > 0$. Under Condition 4.1 it holds

$$\liminf_{\|x\| \rightarrow \infty} \int_{\mathbb{R}^d} q(x, y) \alpha(x, y) dy > 0. \quad (\text{B.16})$$

Proof. Let $w = y - x$ and $\mu_\sigma(w) = \prod_{i=1}^d \mu_\sigma(w_i)$. Also, denote by $\alpha(w; x) = \alpha(x, y)$ the MH acceptance rate when moving from x to y . We write $f(w; x) \gtrsim g(w; x)$ if the function $f(w; x)$ is greater or equal than $g(w; x)$ up to positive constants independent of x and w . From Lemma B.5 we have $\frac{g(1)}{2} \leq Z_i(x) \leq M$ and thus

$$\begin{aligned} q(w; x) \alpha(w; x) &= \frac{\mu_\sigma(w)}{\prod_{i=1}^d Z_i(x)} \min \left\{ \prod_{i=1}^d g(e^{w_i U_i(x)}), e^{U(x+w)-U(x)} \prod_{i=1}^d \frac{g(e^{-w_i U_i(x+w)}) Z_i(x)}{Z_i(x+w)} \right\} \\ &\gtrsim \mu_\sigma(w) \min \left\{ \prod_{i=1}^d g(e^{w_i U_i(x)}), e^{U(x+w)-U(x)} \prod_{i=1}^d g(e^{-w_i U_i(x+w)}) \right\}. \end{aligned}$$

Then, using $g(t) \geq g(1) \min\{1, t\}$ from Lemma B.5 we obtain

$$\begin{aligned} q(w; x) \alpha(w; x) &\gtrsim \mu_\sigma(w) \min \left\{ \prod_{i=1}^d g(e^{w_i U_i(x)}), g(1)^d e^{U(x+w)-U(x)+\sum_{i=1}^d \min\{-w_i U_i(x+w), 0\}} \right\} \\ &\gtrsim \mu_\sigma(w) \min \left\{ \prod_{i=1}^d g(e^{w_i U_i(x)}), e^{U(x+w)-U(x)+\sum_{i=1}^d \min\{-w_i U_i(x+w), 0\}} \right\}. \end{aligned}$$

Assume $\|x\|$ large and $w \in A(x)$, where $A(x) = \{w \in \mathbb{R}^d : \|x+w\| \leq \|x\| - \epsilon, \|w\| \leq 2\epsilon \text{ and } x_i w_i \leq 0 \text{ for all } i\}$ for some fixed $\epsilon > 0$. From $x_i w_i \leq 0$ it follows $w_i U_i(x) \geq 0$ and thus, from the monotonicity of g , $g(e^{w_i U_i(x)}) \geq g(1)$. Combining the latter with the last displayed equation we have

$$q(w; x) \alpha(w; x) \gtrsim \mu_\sigma(w) \min \left\{ g(1)^d, e^{U(x+w)-U(x)+\sum_{i=1}^d \min\{-w_i U_i(x+w), 0\}} \right\}. \quad (\text{B.17})$$

We now lower bound $U(x+w) - U(x) + \sum_{i=1}^d \min\{-w_i U_i(x+w), 0\}$. For $\|x\| > R$, from Condition 4.1

$$\begin{aligned} U(x+w) - U(x) + \sum_{i=1}^d \min\{-w_i U_i(x+w), 0\} &= f(\|x+w\|) - f(\|x\|) + \frac{f'(\|x+w\|)}{\|x+w\|} \sum_{i=1}^d \min\{-w_i(x_i + w_i), 0\}. \end{aligned}$$

Using the non-increasingness of f' and $w \in A(x)$ we have $f(\|x + w\|) - f(\|x\|) \geq -f'(\|x + w\|)(\|x\| - \|x + w\|) \geq -f'(\|x + w\|)\epsilon$. Thus

$$\begin{aligned} U(x + w) - U(x) &+ \sum_{i=1}^d \min\{-w_i U_i(x + w), 0\} \\ &\geq -f'(\|x + w\|) \left(\epsilon + \frac{\sum_{i=1}^d \min\{-w_i(x_i + w_i), 0\}}{\|x + w\|} \right). \end{aligned}$$

Since $w \in A(x)$ it follows $x_i w_i \leq 0$ and $\min\{-w_i(x_i + w_i), 0\} \geq -w_i^2 \geq -(2\epsilon)^2$. Thus

$$\inf_{w \in A(x)} \frac{\sum_{i=1}^d \min\{-w_i(x_i + w_i), 0\}}{\|x + w\|} \geq -\frac{(2\epsilon)^2}{\|x\| - 2\epsilon},$$

which goes to 0 as $\|x\| \rightarrow \infty$. It follows that

$$\begin{aligned} \liminf_{\|x\| \rightarrow \infty} \inf_{w \in A(x)} U(x + w) - U(x) &+ \sum_{i=1}^d \min\{-w_i U_i(x + w), 0\} \geq \\ \liminf_{\|x\| \rightarrow \infty} -f'(\|x\| - 2\epsilon)\epsilon &= \infty. \end{aligned}$$

Combining the last displayed equation with (B.17) we have

$$\liminf_{\|x\| \rightarrow \infty} \inf_{w \in A(x)} q(w; x) \alpha(w; x) \gtrsim \liminf_{\|x\| \rightarrow \infty} \inf_{w \in A(x)} \mu_\sigma(w) > 0,$$

where the last inequality holds for sufficiently small ϵ because of the assumption $\inf_{w \in (-\delta, \delta)} \mu_\sigma(w) > 0$. Therefore

$$\begin{aligned} \liminf_{\|x\| \rightarrow \infty} \int_{\mathbb{R}^d} q(x, y) \alpha(x, y) dy &\geq \liminf_{\|x\| \rightarrow \infty} \int_{A(x)} q(w; x) \alpha(w; x) dw \\ &\gtrsim \liminf_{\|x\| \rightarrow \infty} \int_{A(x)} 1 dw. \end{aligned}$$

The proof is completed noting that $\liminf_{\|x\| \rightarrow \infty} \int_{A(x)} 1 dw > 0$ by the construction of $A(x)$. \square

Proof of Theorem 4.2. Lemmas B.7 and B.8 imply that there exist an $s > 0$ such that V_s satisfy (B.9). The thesis then follows from Lemma B.4, noting that compact sets are small for P (which can be deduced from the fact that $\inf \pi(x) > 0$ on compact sets) and that that $\sup_x QV_s(x)/V_s(x) < \infty$ because

$$\frac{QV_s(x)}{V_s(x)} \leq \sum_{i=1}^d \int_{\mathbb{R}} e^{s|w_i|} q_i(w_i; x) dw_i \leq 2d \int_{\mathbb{R}} e^{s|w_i|} \mu_\sigma(w_i) dw_i < \infty$$

where we used $e^{\|y\|_\infty - \|x\|_\infty} \leq e^{\|y - x\|_\infty} \leq \sum_i e^{|y_i - x_i|}$, $q_i(w_i; x) \leq 2\mu_\sigma(w_i)$ and $\int_{\mathbb{R}} \exp(s|w|) \mu_\sigma(w) dw \leq 2 \int_{\mathbb{R}} \exp(sw) \mu_\sigma(w) dw < \infty$ for every $s > 0$. \square

B.4 Proof of Proposition 4.1

Proposition 4.1 follows directly from Lemmas B.9 and B.10 below.

Lemma B.9. *Under the assumptions of Proposition 4.1 we have*

$$\log \left(\frac{f(x_i + \sigma u_i)}{f(x_i)} \frac{g(e^{-\phi'(x_i + \sigma u_i) \sigma u_i})}{g(e^{\phi'(x_i) \sigma u_i})} \right) = \mathcal{O}(\sigma^3) \quad \text{as } \sigma \rightarrow 0, \quad (\text{B.18})$$

for all $x_i, w_i \in \mathbb{R}$.

Proof. Define the function b as $b(s) = \log(g(\exp(s)))$ for all $s \in \mathbb{R}$. For any x_i, u_i in \mathbb{R} , we have

$$\begin{aligned} & \log \left(\frac{f(x_i + \sigma u_i)}{f(x_i)} \frac{g(e^{-\phi'(x_i + \sigma u_i)\sigma u_i})}{g(e^{\phi'(x_i)\sigma u_i})} \right) \\ &= \phi(x_i + \sigma u_i) - \phi(x_i) + b(-\phi'(x_i + \sigma u_i)\sigma u_i) - b(\phi'(x_i)\sigma u_i) \\ &= c_1(x_i)\phi'(x_i)u_i\sigma + c_2(x_i)\frac{u_i^2\sigma^2}{2} + c_3(x_i)\frac{u_i^3\sigma^3}{6} + \mathcal{O}(\sigma^4) \quad \text{as } \sigma \rightarrow 0, \end{aligned} \quad (\text{B.19})$$

where $c_1(x_i)$ and $c_2(x_i)$ are the coefficients of the second order Taylor expansion about $\sigma = 0$, and are given by $c_1(x_i) = (1 - 2b'(0))\phi'(x_i)$ and $c_2(x_i) = (1 - 2b'(0))\phi''(x_i)$. To conclude, we now show that the assumptions on g imply $b'(0) = 1/2$ and $c_1(x_i) = c_2(x_i) = 0$. By definition of b it holds that $b'(0) = g'(1)/g(1)$. From $g(t) = t g(1/t)$ it follows $g(1 + \epsilon) = (1 + \epsilon) g((1 + \epsilon)^{-1})$ and thus $\frac{g(1+\epsilon) - g((1+\epsilon)^{-1})}{2\epsilon} = \frac{g((1+\epsilon)^{-1})}{2}$. Taking the limit $\epsilon \downarrow 0$ and using $(1 + \epsilon)^{-1} = 1 - \epsilon + \mathcal{O}(\epsilon^2)$ it follows that $g'(1) = \frac{g(1)}{2}$ and thus $b'(0) = 1/2$ and $c_1(x_i) = c_2(x_i) = 0$. Combining the latter with (B.19) we obtain (B.18). \square

Remark B.1. For general ϕ , x_i and u_i , we have $\log(\alpha_i(x_i, x_i + \sigma u_i)) = \Theta(\sigma^3)$ because the third coefficient in the Taylor expansion in (B.19), which is given by

$$c_3(x_i) = 6b''(0)\phi'(x_i)\phi''(x_i) - 2b'''(0)\phi'(x_i)^3 + (1 - 3b'(0))\phi'''(x_i),$$

is non-zero in general.

Lemma B.10. Under the assumptions of Proposition 4.1 we have

$$\log \left(\frac{Z_i(x_i)}{Z_i(x_i + \sigma u_i)} \right) = \mathcal{O}(\sigma^3) \quad \text{as } \sigma \rightarrow 0,$$

for all $x_i, w_i \in \mathbb{R}$.

Proof. Without loss of generality, assume $g(1) = 1$ throughout the proof. First consider $\log(Z_i(x_i))$, which can be written as

$$Z_i(x_i) = \int_{\mathbb{R}} g(e^{\phi'(x_i)(y_i - x_i)}) \sigma^{-1} \mu\left(\frac{y_i - x_i}{\sigma}\right) dy_i = \int_{\mathbb{R}} g(e^{\phi'(x_i)\sigma s}) \mu(s) ds. \quad (\text{B.20})$$

For every non-negative integer j , denote by κ_j the j -th moment of the distribution $\mu(\cdot)$. Note that, since μ is a symmetric pdf, $\kappa_0 = 1$, $\kappa_j = 0$ if j is odd and $\kappa_j > 0$ if j is even. For $j \in \{1, 2, 3\}$, we have

$$\begin{aligned} \frac{\partial^j}{\partial \sigma^j} Z_i(x_i) \Big|_{\sigma=0} &= \int_{\mathbb{R}} \frac{\partial^j}{\partial \sigma^j} g(e^{\phi'(x_i)\sigma s}) \Big|_{\sigma=0} \mu(s) ds = \\ &= \int_{\mathbb{R}} \frac{\partial^j}{\partial \sigma^j} g(e^{\phi'(x_i)\sigma}) \Big|_{\sigma=0} s^j \mu(s) ds = \frac{\partial^j}{\partial \sigma^j} g(e^{\phi'(x_i)\sigma}) \Big|_{\sigma=0} \kappa_j, \end{aligned} \quad (\text{B.21})$$

where the exchange of integration and derivation is justified by the assumptions on g and μ . Using the Taylor expansion of the function $\sigma \mapsto \log(h(\sigma))$ for general h about $\sigma = 0$, and the fact that $Z_i(x_i) \Big|_{\sigma=0} = 1$ and $\frac{\partial^j}{\partial \sigma^j} Z_i(x_i) \Big|_{\sigma=0} = 0$ if j is odd, we have

$$\begin{aligned} \log(Z_i(x_i)) &= \kappa_2 \frac{\partial^2}{\partial \sigma^2} g(e^{\phi'(x_i)\sigma}) \Big|_{\sigma=0} \frac{\sigma^2}{2} + \mathcal{O}(\sigma^4) \\ &= \kappa_2 (g'(1) + g''(1)) \phi'(x_i)^2 \frac{\sigma^2}{2} + \mathcal{O}(\sigma^4) \quad \text{as } \sigma \rightarrow 0. \end{aligned} \quad (\text{B.22})$$

Set $y_i = x_i + \sigma u_i$, then from (B.20) and (B.21)

$$\frac{\partial^j}{\partial \sigma^j} Z_i(x_i + \sigma u_i) \Big|_{\sigma=0} = \int_{\mathbb{R}} \frac{\partial^j}{\partial \sigma^j} g \left(e^{\phi'(x_i + \sigma u_i) \sigma s} \right) \Big|_{\sigma=0} \mu(s) ds$$

Reordering the Taylor expansion of $g \left(e^{\phi'(x_i + \sigma u_i) \sigma s} \right)$ about $\sigma = 0$ as a polynomial of s and keeping only even powers in s we get

$$Z_i(x_i + \sigma u_i) = 1 + \kappa_2(g'(1) + g''(1))\phi'(x_i)^2 \frac{\sigma^2}{2} + \mathcal{O}(\sigma^3).$$

Using the expansion of $\log(h(\sigma))$ for general h about $\sigma = 0$, and the fact that $Z_i(x_i + \sigma u_i) \Big|_{\sigma=0} = 1$ and $\frac{\partial}{\partial \sigma} Z_i(x_i + \sigma u_i) \Big|_{\sigma=0} = 0$, we have

$$\log(Z_i(x_i + \sigma u_i)) = \kappa_2(g'(1) + g''(1))\phi'(x_i)^2 \frac{\sigma^2}{2} + \mathcal{O}(\sigma^3).$$

Combining the latter equation with (B.22) we have

$$\log \left(\frac{Z_i(x_i)}{Z_i(x_i + \sigma u_i)} \right) = \log(Z_i(x_i)) - \log(Z_i(x_i + \sigma u_i)) = +\mathcal{O}(\sigma^3)$$

□

Remark B.2. For the Barker proposal, the normalization term $Z_i(x_i)$ is constant over x_i and thus Lemma B.10 is trivially satisfied.

C Condition 2.3 for the exponential family class

Proposition C.1. Condition 2.3 holds in the case in which there are $\alpha, \beta > 0$ such that

$$\pi(x) \propto \exp\{-\alpha \|x\|^\beta\}$$

Proof. Condition (ii) is immediate. For (i), first note that here

$$\left| \frac{\partial \log \pi(x)}{\partial x_1} \right| \|x\|^\gamma = -\alpha \beta x_1 \|x\|^{\gamma+\beta-2}. \quad (\text{C.1})$$

Note that $\|x\| = \sqrt{(\sum_i x_i^2)}$ is a monotonically increasing function in each $|x_i|$, so the infimum over (x_2, \dots, x_d) of (C.1) is realised at $x_2 = \dots = x_d = 0$. Choosing $\gamma = 2$ condition (i) is satisfied because

$$\liminf_{|x_1| \rightarrow \infty} \alpha \beta |x_1|^{1+\beta} = \infty.$$

□

D Locally balanced proposals and skew-symmetric distributions

In this section we show that the only balancing function g leading to a skew-symmetric distribution is $g(t) = \frac{t}{1+t}$. Following [Azzalini, 2013], a skew-symmetric distribution on \mathbb{R} is distribution for which the probability density can be written

$$f(z) = 2f_0(z)G(z),$$

for any $z \in \mathbb{R}$, where $f_0(z) = f_0(-z)$, $G(z) \geq 0$ and

$$G(z) + G(-z) = 1. \quad (\text{D.1})$$

In the first-order locally-balanced framework, if the current point is x then the proposal has density

$$f_x(z) = Z(x)^{-1} \mu_\sigma(z) g(e^{\nabla \log \pi(x)z}),$$

where, setting $t = e^{\nabla \log \pi(x)z}$ the balancing function g satisfies

$$g(t) = tg(1/t). \quad (\text{D.2})$$

Equating (D.1) and (D.2) gives $G(z) = g(e^{\nabla \log \pi(x)z}) = g(t)$, implying that in this case

$$G(-z) = g(1/t).$$

Therefore, dividing (D.1) by $G(1/z)$, using the above and combining with (D.2) gives

$$t + 1 = \frac{1}{g(1/t)},$$

and combining with (D.2) gives

$$g(t) = \frac{t}{1+t}.$$

as required.

E Pre-conditioning the Barker proposal

The diagonal non-isotropic version of the Barker scheme is a simple variation of Algorithm 2 from the paper and is described in Algorithm 3. The acceptance probability related to Algorithm

Algorithm 3 Diagonal Barker proposal on \mathbb{R}^d

Require: current point $x \in \mathbb{R}^d$ and local scales $(\sigma_1, \dots, \sigma_d) \in (0, \infty)^d$

Independently for each $i \in \{1, \dots, d\}$ do:

1. Draw $z_i \sim \mu_{\sigma_i}$
2. Calculate $p_i(x, z_i) = 1/(1 + e^{-z_i \partial_i \log \pi(x)})$
3. Set $b_i(x, z_i) = 1$ with probability $p_i(x, z_i)$, and $b_i(x, z_i) = -1$ otherwise
4. Set $y_i = x_i + b_i(x, z_i) \times z_i$

Output: the resulting proposal y .

3 is exactly the same $\alpha^B(x, y)$ defined in (3.5) of the paper.

The preconditioned version of the Barker algorithm is obtained by defining an appropriate linear transformation to the target variables x and then applying the standard Barker algorithm (Algorithm 2 from the paper) in the transformed space. More precisely, given a target π and a covariance matrix Σ with Cholesky decomposition C , define the transformed variables $\tilde{x} = (C^T)^{-1}x$ with distribution $\tilde{\pi}(\tilde{x}) \propto \pi(C^T \tilde{x})$ and log-gradient $\nabla \log \tilde{\pi}(\tilde{x}) = \nabla \log \pi(C^T \tilde{x}) \cdot C^T$, where \cdot denotes vector-matrix multiplication, and then apply the Barker algorithm described in Algorithm 2 of the paper to $\tilde{\pi}$. The resulting scheme can be implemented without explicitly defining the auxiliary variables \tilde{x} and is described in Algorithms 4 and 5. In the following $c(x) = \nabla \log \pi(x) \cdot C^T$ represents the preconditioned gradient.

Algorithm 4 Preconditioned Barker proposal on \mathbb{R}^d

Require: current point $x \in \mathbb{R}^d$ and preconditioning matrix $C = chol(\Sigma)$.

1. Draw $z_i \sim \mu$ independently for each $i \in \{1, \dots, d\}$
2. Calculate $p_i(x, z) = 1/(1 + e^{-z_i c_i(x)})$ where $c_i(x) = (\nabla \log \pi(x) \cdot C^T)_i$
3. For each i , set $\tilde{z}_i = z_i$ with probability $p_i(x, z)$, and $\tilde{z}_i = -z_i$ otherwise
4. Set $y = x + C^T \tilde{z}$ where $\tilde{z} = (\tilde{z}_1, \dots, \tilde{z}_d)$

Output: the resulting proposal y .

Algorithm 5 Metropolis–Hastings with preconditioned Barker proposal

Require: starting point for the chain $x^{(0)} \in \mathbb{R}$, and preconditioning matrix $C = chol(\Sigma)$.
Set $t = 0$ and do the following:

1. Given $x^{(t)} = x$, draw y using Algorithm 4 and compute

$$\alpha^B(x, y) = \min \left(1, \frac{\pi(y)}{\pi(x)} \times \prod_{i=1}^d \frac{1 + e^{-z_i c_i(x)}}{1 + e^{z_i c_i(y)}} \right).$$

where $z_i = ((C^T)^{-1}(y - x))_i$ and $c(x) = (\nabla \log \pi(x) \cdot C^T)_i$

2. Set $x^{(t+1)} = y$ with probability $\alpha^B(x, y)$, and $x^{(t+1)} = x$ otherwise
3. If $i + 1 < N$, set $i \leftarrow i + 1$ and return to step 1, otherwise stop.

Output: the Markov chain $\{x^{(0)}, \dots, x^{(N)}\}$.

F Additional figures for simulations

F.1 Illustrations of robustness to heterogeneity

In Figure 8 we display a phenomenon analogous to Figure 2 of the paper on a 20-dimensional example in which each component of $\pi(\cdot)$ is an independent $N(0, \eta_i^2)$ random variable, with $\eta_1 = 0.01$ and $\eta_i = 1$ for $i = 2, \dots, 20$. Here the performance of MALA starts deteriorating drastically as soon as the step-size exceeds the scale of the first component as we would expect from the theory developed in Section 2 of the paper. On the other hand both the random walk and Barker schemes can function adequately with larger than optimal step-sizes, and as a result achieve a much higher expected squared jump distance on all the other coordinates.

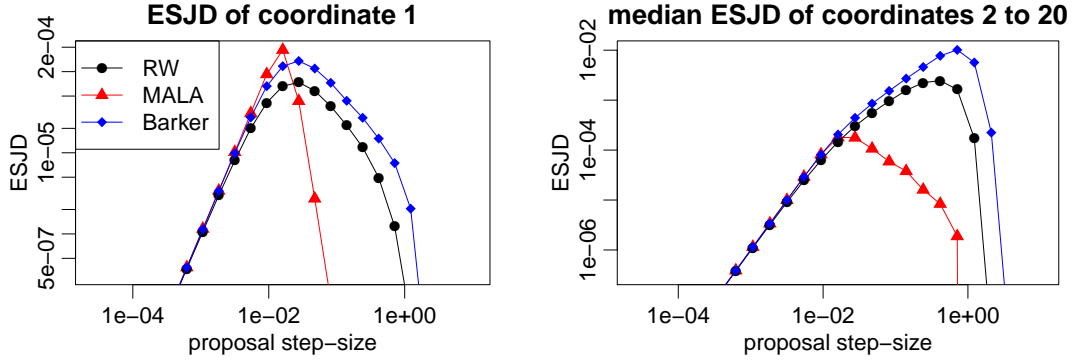


Figure 8: Expected squared jump distance (ESJD) against proposal step-size for RW, MALA and Barker on a 20-dimensional target in which one component has a smaller scale than all others.

F.2 Implications for adaptive MCMC

In Figures 9 to 12 we repeat experiments performed in Section 5.2 with different choices of learning rate $\gamma_t := t^{-\kappa}$. In Figure 9 we consider the setting in which the scale of the first component is smaller than that of all others, coinciding with the theoretical sections of the paper, set $\kappa = 0.8$, and find that with this choice the local scales fail to settle on sensible values in the MALA case. Performance is relatively unchanged for the random walk and Barker schemes. In Figure 10 we set $\kappa = 0.4$. In this case the adaptation process is slightly less stable for all algorithms, particularly the local scales of the random walk algorithm and the global scale of MALA, but MALA does eventually begin to behave sensibly after around 7000 iterations. In this example, smaller values of κ led to instability for MALA. The same features are true of Figures 11 and 12, in which the log-scales of the target distribution are sampled from a $N(0, 3^2)$ distribution.

F.3 Additional simulations for the crossed random effects model

In Figures 13 to 16 we performed further experiments on the crossed random effect example of Section 5.4. First we tried changing the parameter κ that governs the learning schedule of the Robbins-Monroe algorithm used in the adaptation procedure. The results, which are reported in Figures 13 and 14, display no significant improvements in the behaviour of the algorithms, but a minor improvement in the random walk case in Figure 13.

Second we tried starting the algorithms from the mode of the target distribution (found numerically with optimization algorithms) and also initializing the proposal covariance to the inverse of the negative hessian of the log target density evaluated at the mode. As shown in Figure 15, starting from the mode reduced, though modestly, the time required for the

adaptation phase. Somewhat surprisingly, the performance of algorithms was slightly worse when starting the covariance adaptation using the inverse hessian (Figure 16).

F.4 Comparison to Hamiltonian Monte Carlo

Figure 17 shows the trace plots of μ , a_1 and b_1 obtained with the Stan implementation of the No-U-Turn Sampler (NUTS), both in the default version in which a diagonal covariance/mass matrix is learned during the adaptation process, and using the dense mass matrix option. Both versions are run for 10^4 iterations. The diagonal version required around 55 leapfrog steps per iteration, corresponding to over 10^6 gradient evaluations in total. In terms of gradient evaluations, this is roughly comparable to 5×10^5 iterations of MALA or Barker. The dense version requires around 955 leapfrog steps per iteration, corresponding to roughly 2×10^7 gradient evaluations and 10^7 iterations of MALA or Barker. In terms of convergence and mixing, the diagonal version looks to converge to the correct posterior but exploration of this distribution is slow. For example, after removing the first half of the samples as burn-in, the effective sample size per gradient evaluation for the parameter μ is estimated to be 46.2, which is roughly three orders of magnitude worse than the effective sample size per gradient evaluation obtained when using the Barker scheme, shown in Figure 7. The version of NUTS with a dense mass matrix appears to exhibit unstable behavior and fails to converge to the region of high-posterior mass. It should be noted that caution is recommended when using the dense mass matrix setting within the Stan software, as it is acknowledged that learning such an object during sampling can be a challenge for the algorithm.

F.5 Comparison to truncated or tamed gradients

Consider Metropolis–Hastings proposals of the form

$$y = x + \frac{\sigma^2}{2}G(x) + \sigma\xi,$$

for some $\sigma > 0$, $G : \mathbb{R}^d \rightarrow \mathbb{R}^d$ and $\xi \sim N(0, I)$. Setting $G(x) = \nabla \log \pi(x)$ leads to the MALA proposal. A common way to improve the stability of MALA in the literature is to truncate or tame the gradient $\nabla \log \pi(x)$. For example, in the truncated MALA algorithm (MALTA) [Atchade, 2006] we have

$$G(x) = \frac{\delta}{\max\{\delta, \|\nabla \log \pi(x)\|\}} \nabla \log \pi(x),$$

for some $\delta > 0$, while in the component-wise tamed MALA (MALTAc) [Brosse et al., 2018, eq.(4)] the function $G(x) = (G_1(x), \dots, G_d(x))$ is defined component-wise as

$$G_i(x) = \frac{\partial_i(x)}{1 + \sigma^2|\partial_i(x)|}.$$

Such schemes are effective in achieving geometric ergodicity also for light tails [Atchade, 2006]. They are less effective, however, in terms of being robust to heterogeneity, as shown in Figures 18-20. There we compare MALTA, MALTAc and Barker on the target considered in Figure 4 of the main paper. For MALTA we set $\delta = 1000$, as is done for example, in Atchade [2006]. We also tried setting $\delta = 100$ without observing much of a difference. Figure 18 considers exactly the same target of Figure 4 of the paper. We see that both MALTA and MALTAc improve over MALA, and in particular that MALTAc manages to converge to stationarity in around 4000 iterations, although this is still significantly slower than Barker (which only requires few hundred iterations).

Crucially, however, both MALTA and MALTA_c are sensitive to the choice of truncation parameter (respectively δ and σ^{-2}). As a consequence they can perform very differently depending on the scales of the target distribution. In Figures 19 and 20 we consider the same target distribution of 19, and multiply (Figure 19) or divide (Figures 20) the scales of all coordinates by 100. The performances of MALTA and MALTA_c deteriorate dramatically, while the performance of the Barker scheme is essentially unchanged.

Finally, in Figure 21 we compare MALTA, MALTA_c and Barker on the crossed random effect example of Section 5.4 of the paper, under the same setting as that of Figure 7. Here MALTA and MALTA_c perform poorly and fail to converge to stationarity in 500,000 iterations, while the Barker scheme performs well as described in Section 5.4 of the main paper.

These results suggest that ad-hoc strategies to improve the robustness of gradient-based MCMC, such as truncating or taming gradients, are intrinsically more fragile and sensitive to heterogeneity and scales compared to a more principled solution such as the Barker algorithm, in which robustness arises naturally from the proposal mechanism. In addition to this, truncating and taming can be thought of as introducing a ‘bias’ into the proposal mechanism, in the sense that the resulting proposal is no longer first-order exact, and this typically compromises the $d^{-1/3}$ scaling behaviour.

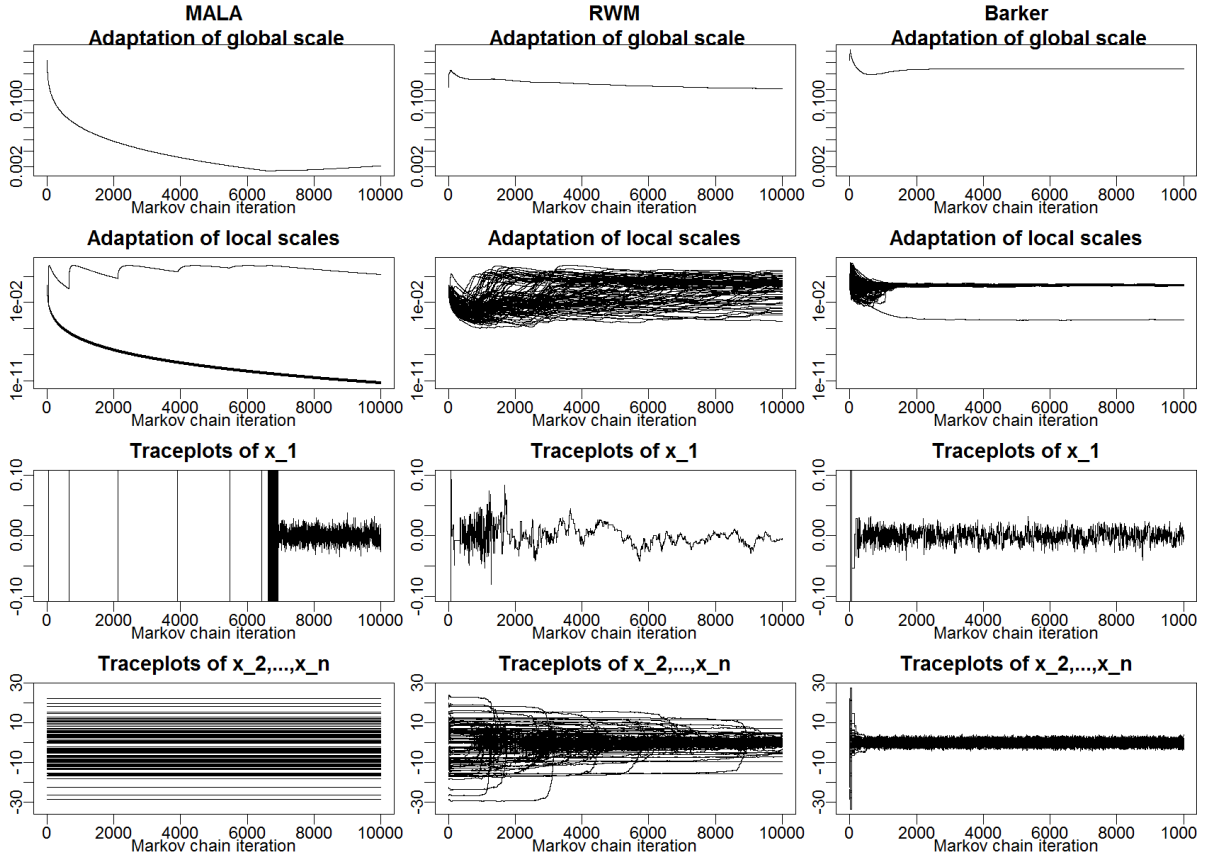


Figure 9: Same setting as in Figure 4 from the paper with $\kappa = 0.8$.

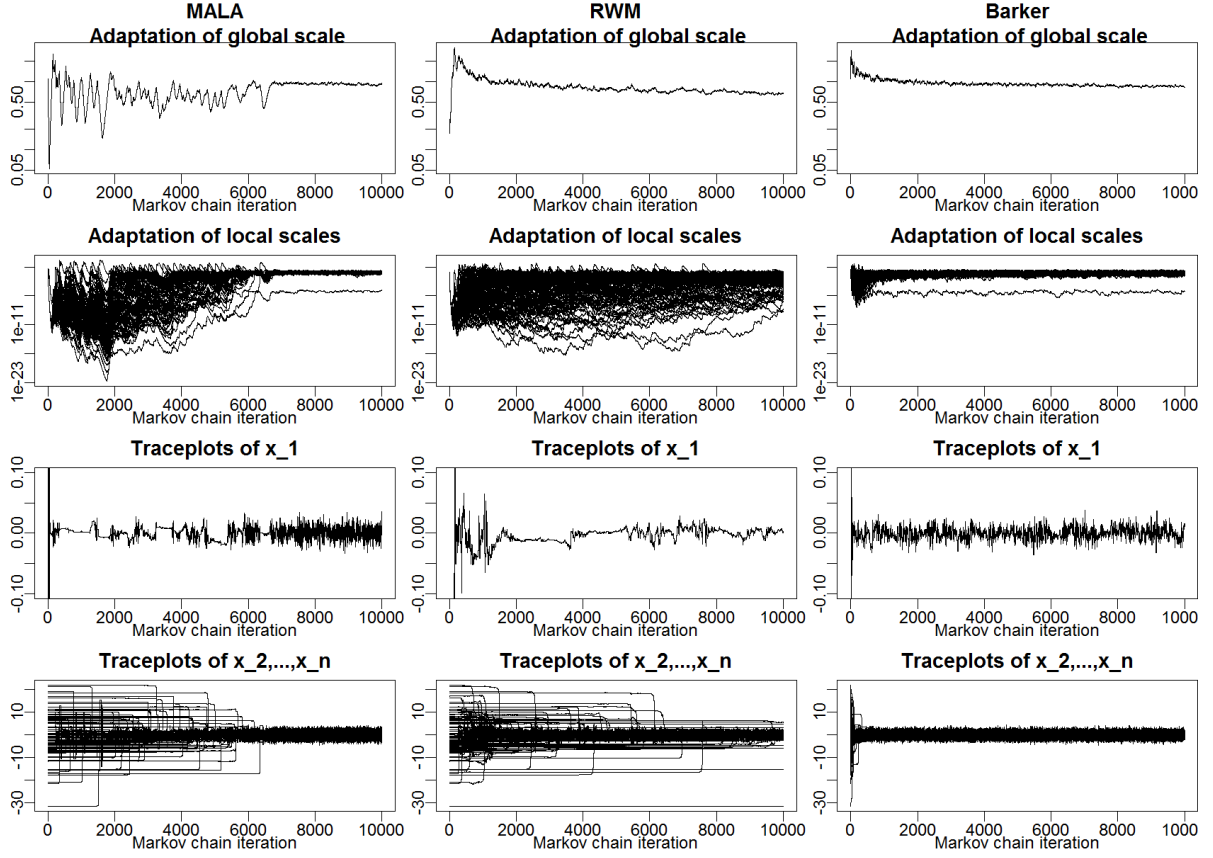


Figure 10: Same setting as in Figure 4 from the paper with $\kappa = 0.4$.

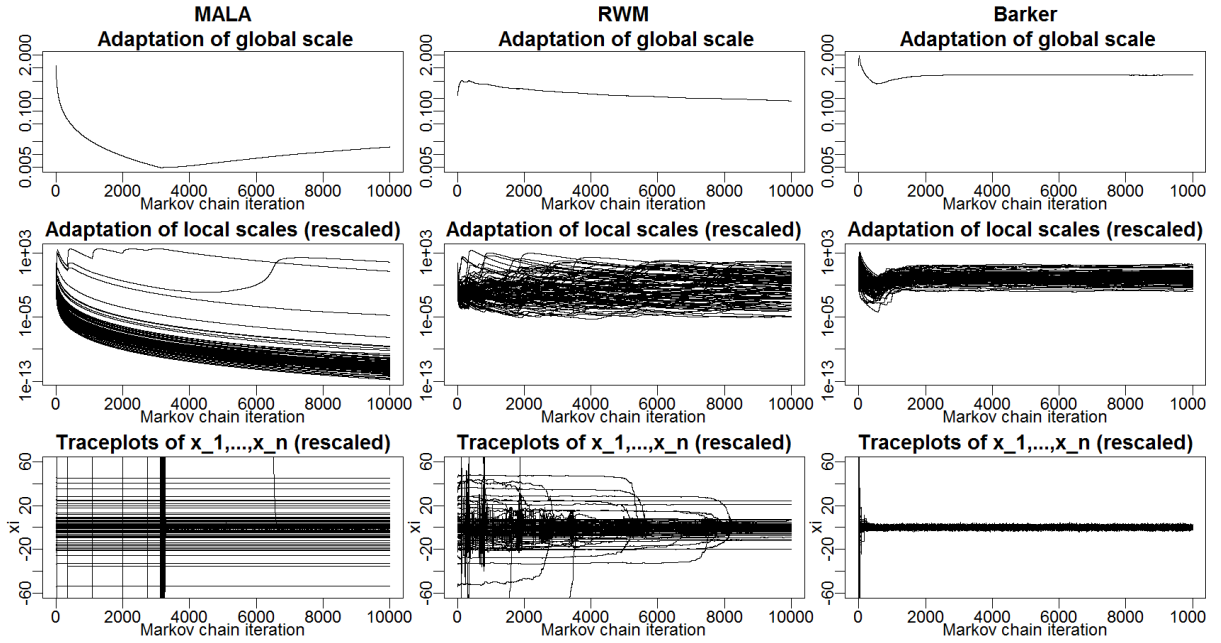


Figure 11: As in Figure 11 from the paper with $\kappa = 0.8$.

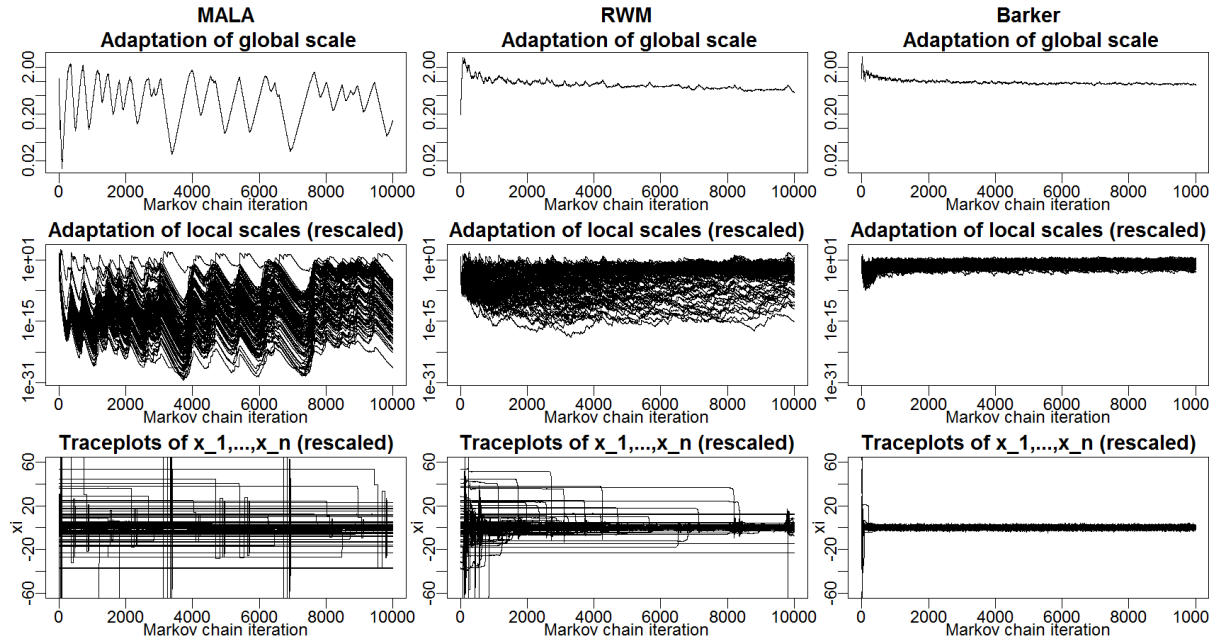


Figure 12: As in Figure 11 from the paper with $\kappa = 0.4$.

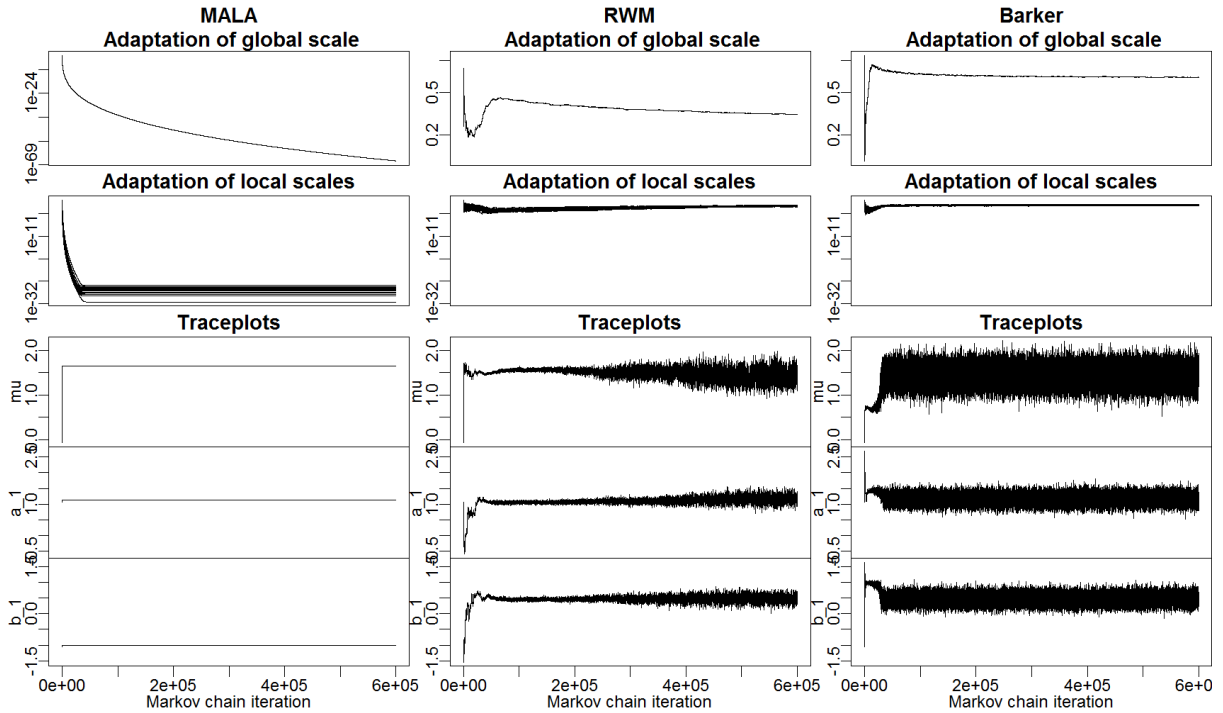


Figure 13: As in Figure 7 but with $\kappa = 0.7$ (plus some regularization of the covariance to avoid numerical issues). We see a minor improvement for RW but otherwise the same pattern as in Figure 7.

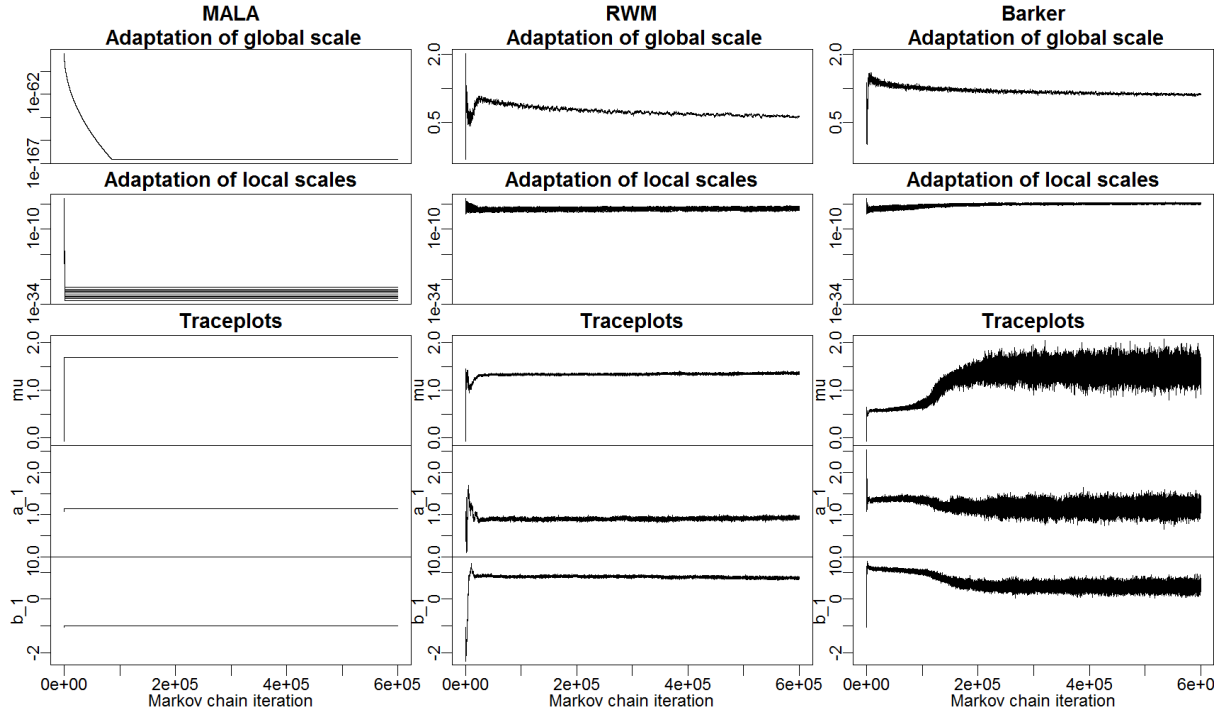


Figure 14: As in Figure 7 but with $\kappa = 0.5$ (plus some regularization of the covariance to avoid numerical issues). Here the performances for both RW and Barker are worse than in Figure 7.

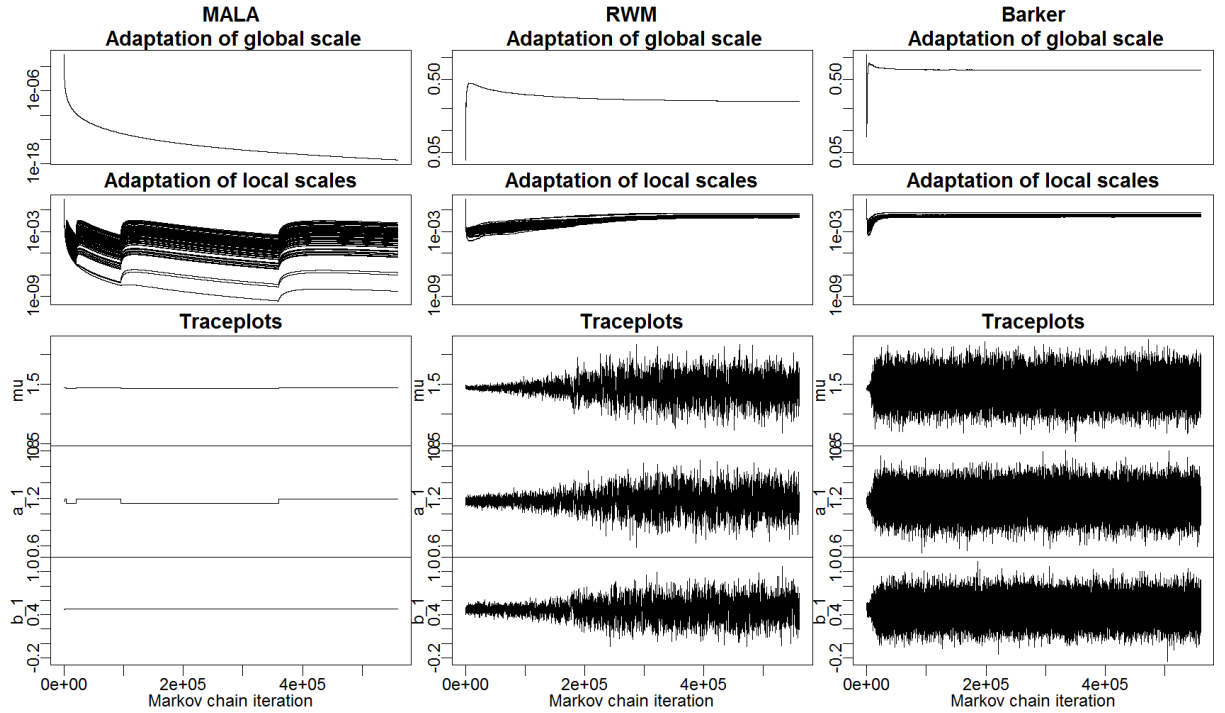


Figure 15: As in Figure 7 but with algorithms initialised at the posterior mode, which is computed with the BFGS algorithm implemented in the *optim* R function (the default version of *optim* with the Nelder-Mead algorithm returned a worse starting point).

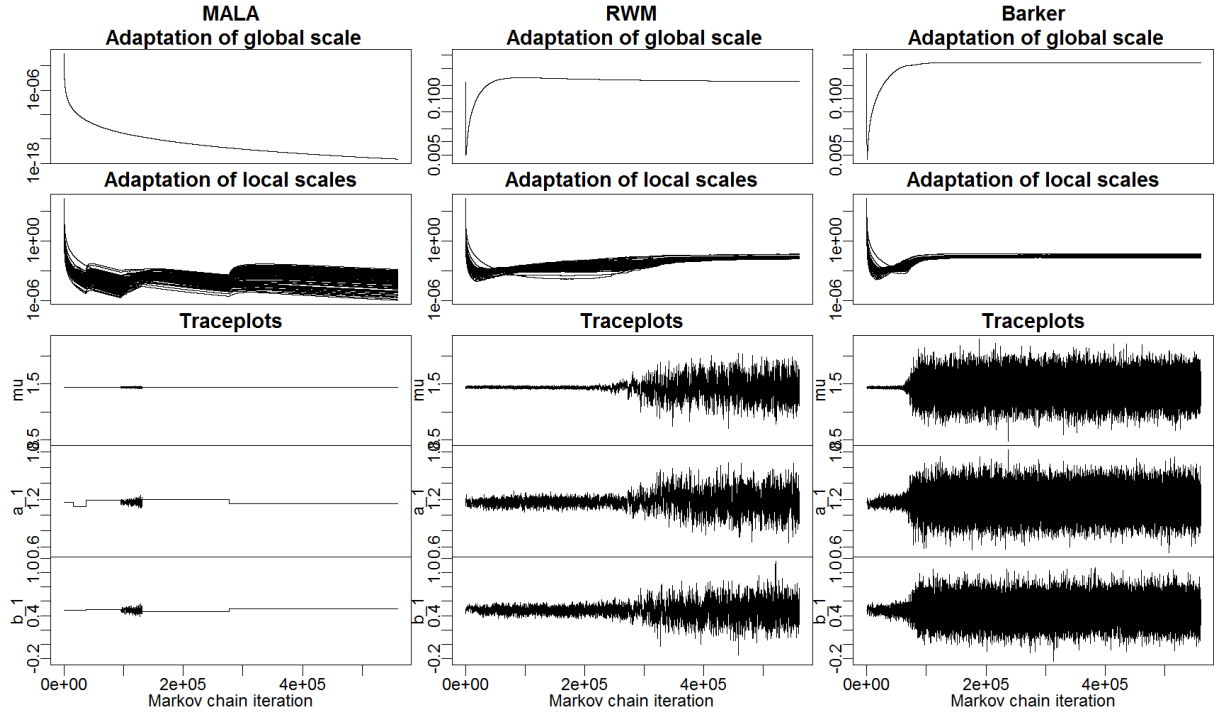


Figure 16: As in Figure 7 but with algorithms initialised at the posterior mode and Σ_0 set to be the inverted Hessian of the log-posterior evaluated at the mode. Both the mode and hessian are computed with the *optim* R function as for Figure 15.

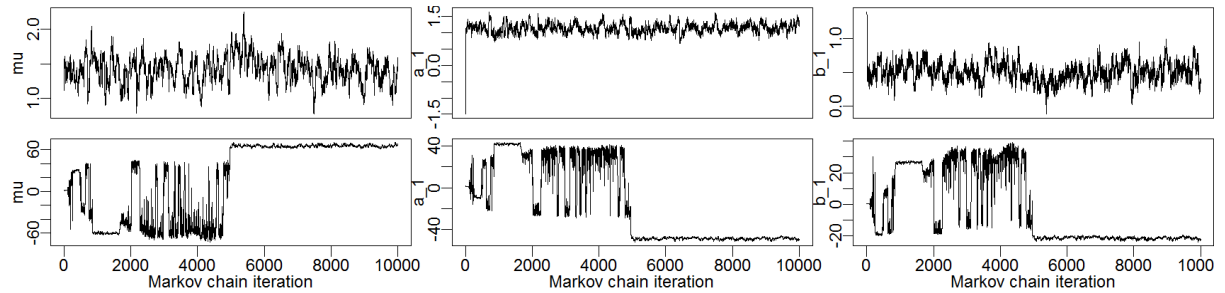


Figure 17: Sampling from the same posterior as in Figure 7 using the Stan implementation of NUTS with diagonal adaptation (first row) and dense covariance adaptation (second row). The version with dense covariance is unstable and fails to converge to the correct posterior.

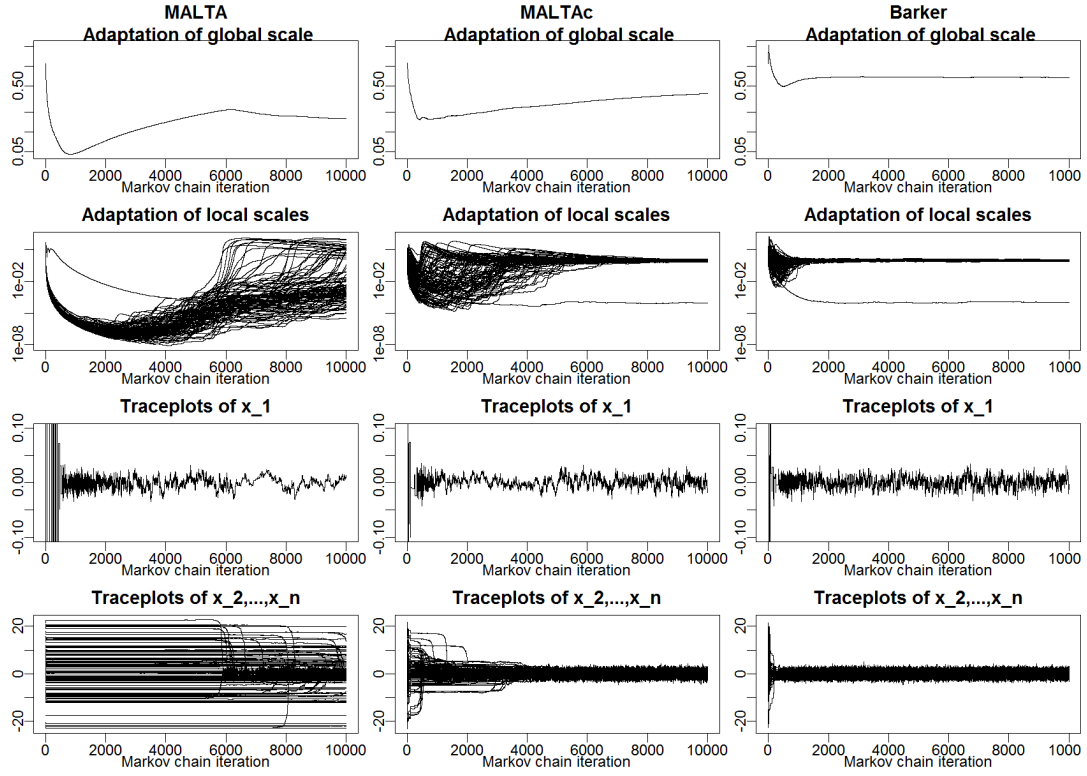


Figure 18: Comparison of MALTA, MALTAc and Barker on the target considered in Figure 4 of the paper (100-dimensional Gaussian with first component standard deviation equal to 0.01 and all others standard deviations equal to 1).

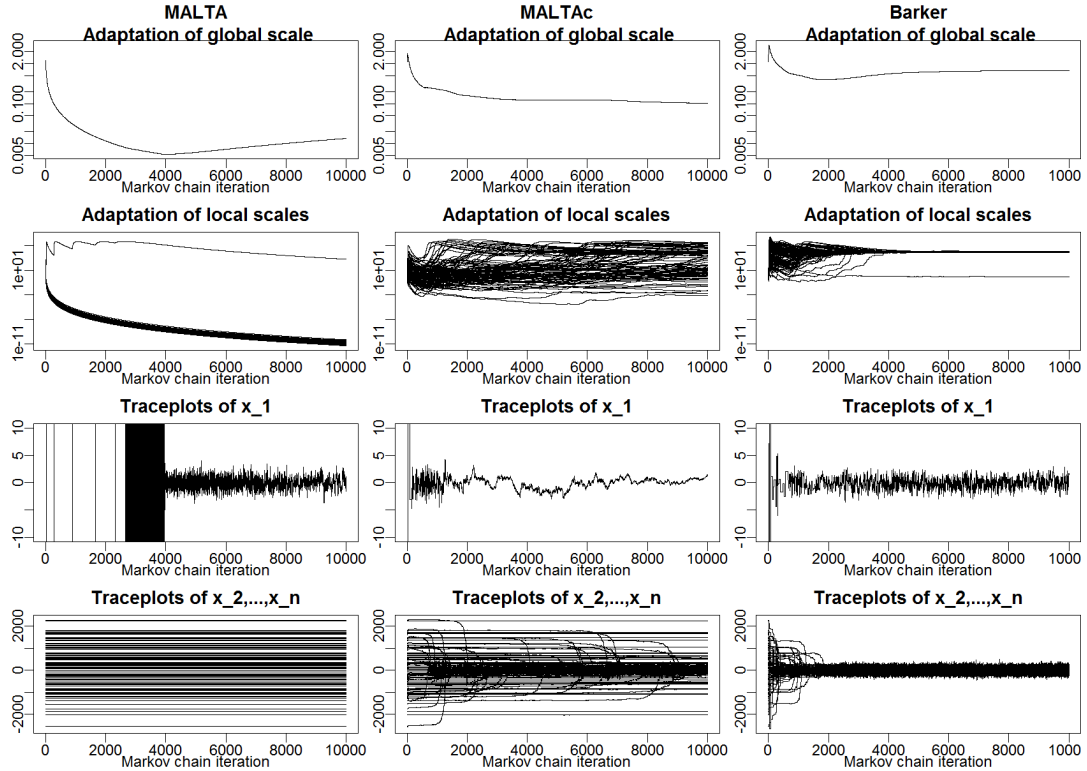


Figure 19: Comparison of MALTA, MALTAc and Barker on a re-scaled version of the target in Figure 18 (100-dimensional Gaussian with the first component standard deviation equal to 1 and all others standard deviations equal to 100).

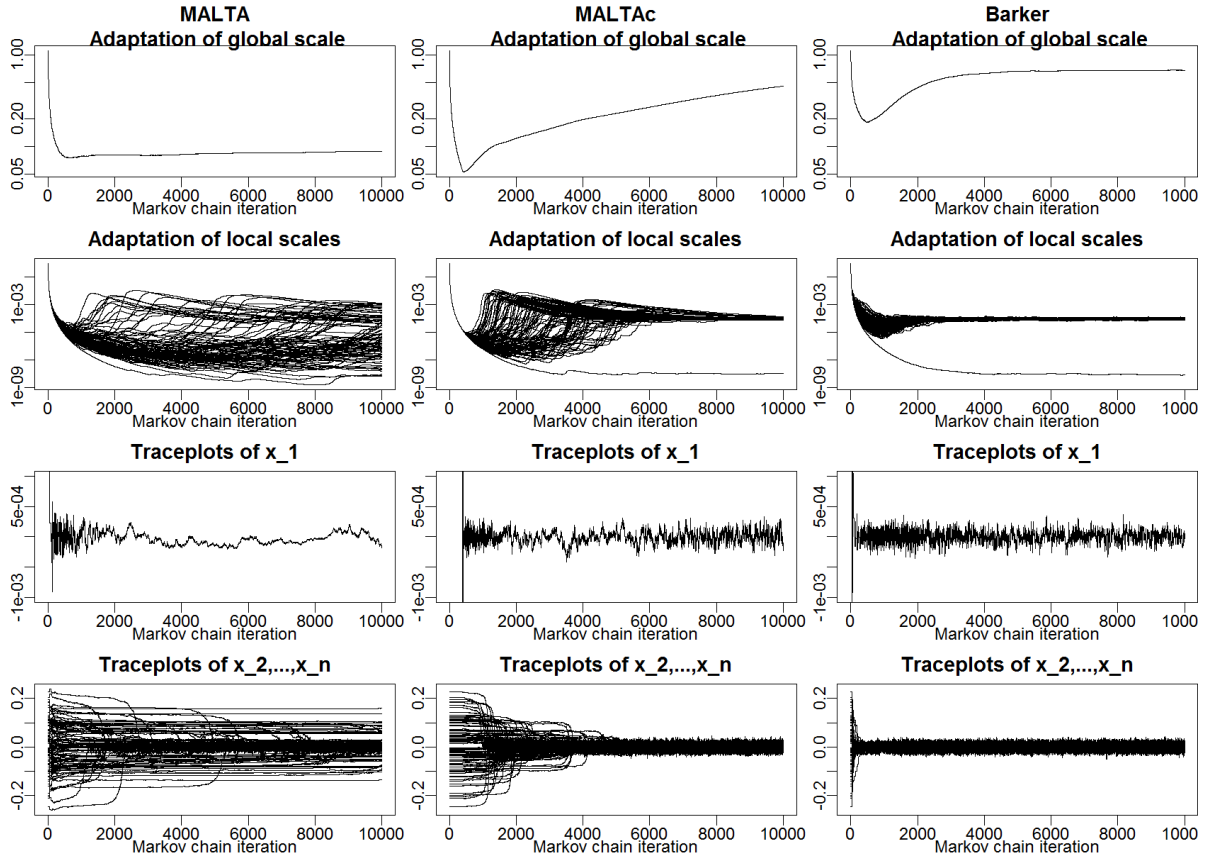


Figure 20: Comparison of MALTA, MALTAc and Barker on a re-scaled version of the target in Figure 18 (100-dimensional Gaussian with the first component standard deviation equal to 0.0001 and all others standard deviations equal to 0.01).

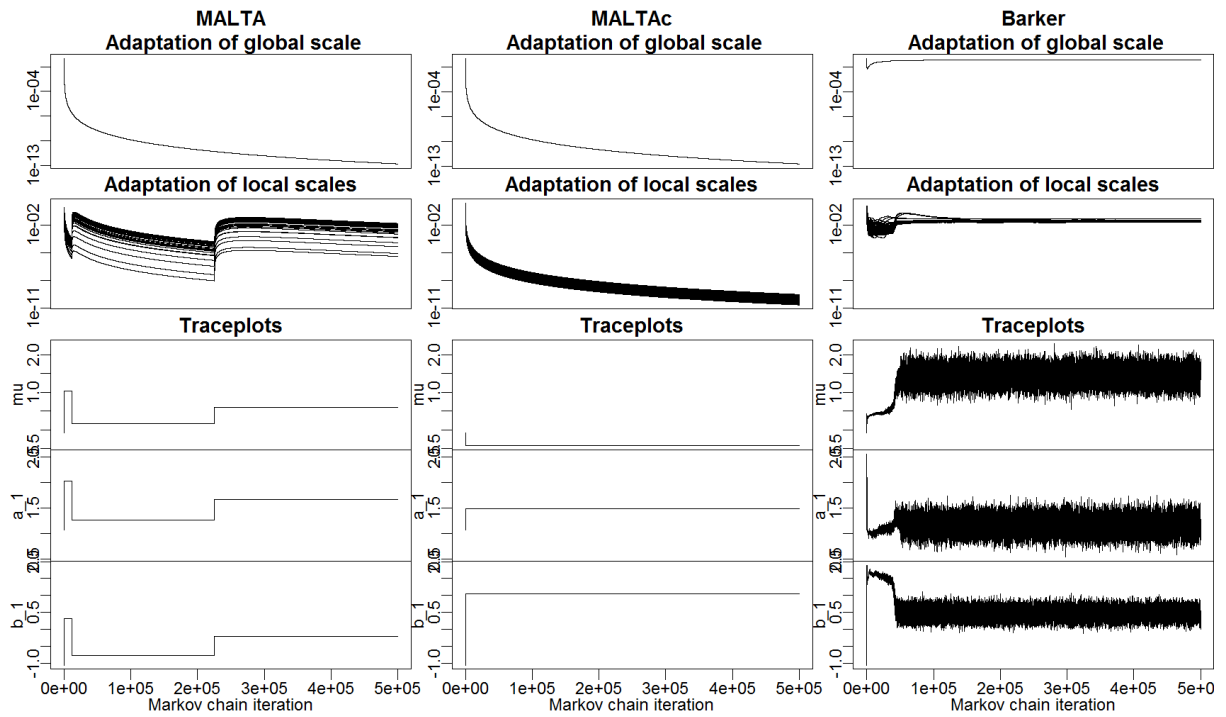


Figure 21: Comparison of MALTA, MALTAc and Barker on the posterior distribution considered in Figure 7 of the paper.